Article

Secreted fungal virulence effector triggers allergic inflammation via TLR4

https://doi.org/10.1038/s41586-022-05005-4

Received: 15 September 2021

Accepted: 21 June 2022

Published online: 27 July 2022

Check for updates

Eric V. Dang[1], Susan Lei[1], Atanas Radkov[1], Regan F. Volk[2,3], Balyn W. Zaro[2,3] & Hiten D. Madhani[1,4]✉

Invasive fungal pathogens are major causes of human mortality and morbidity[1,2]. Although numerous secreted effector proteins that reprogram innate immunity to promote virulence have been identified in pathogenic bacteria, so far, there are no examples of analogous secreted effector proteins produced by human fungal pathogens. *Cryptococcus neoformans*, the most common cause of fungal meningitis and a major pathogen in AIDS, induces a pathogenic type 2 response characterized by pulmonary eosinophilia and alternatively activated macrophages[3–8]. Here, we identify CPL1 as an effector protein secreted by *C. neoformans* that drives alternative activation (also known as M2 polarization) of macrophages to enable pulmonary infection in mice. We observed that CPL1-enhanced macrophage polarization requires Toll-like receptor 4, which is best known as a receptor for bacterial endotoxin but is also a poorly understood mediator of allergen-induced type 2 responses[9–12]. We show that this effect is caused by CPL1 itself and not by contaminating lipopolysaccharide. CPL1 is essential for virulence, drives polarization of interstitial macrophages in vivo, and requires type 2 cytokine signalling for its effect on infectivity. Notably, *C. neoformans* associates selectively with polarized interstitial macrophages during infection, suggesting a mechanism by which *C. neoformans* generates its own intracellular replication niche within the host. This work identifies a circuit whereby a secreted effector protein produced by a human fungal pathogen reprograms innate immunity, revealing an unexpected role for Toll-like receptor 4 in promoting the pathogenesis of infectious disease.

Invasive fungal pathogens are responsible[2] for approximately 1.5 million deaths per year. They account for 50% of AIDS-related deaths and have been referred to as a 'neglected epidemic'[1]. New, drug-resistant fungal pathogens have been identified[13], and available drugs display limited efficacy and high toxicity[14]. Despite these challenges, how fungal pathogens evade host immunity to replicate and cause disease is incompletely understood. Fungal pathogens of plants use secreted effector proteins to thwart plant immune systems to enable infection[15]. Although secretion of immunomodulatory effector proteins could be a strategy for fungi to drive infection in mammals, such molecules have yet to be identified. *C. neoformans* is an environmental yeast that is acquired by inhalation and subsequently causes lethal meningitis in immunocompromised individuals[3]. It is the most common cause of fungal meningitis, and Cryptococcal infection results in fatality in between 10% and 70% of cases and around 200,000 deaths annually[16]. During infection of mice, *C. neoformans* induces a type 2 immune response that is detrimental to host protection[5,7,8,17,18]. Despite the importance of skewed immune responses on pulmonary infection outcome, little is known about how *C. neoformans* promotes type 2 inflammation.

Macrophage polarization by *C. neoformans*

Production of a polysaccharide capsule helps *C. neoformans* evade phagocytosis by macrophages[19]. Capsular polysaccharides may have additional immunomodulatory functions[20]. To test whether the capsule contributes to suppression of macrophage activation, we measured tumour necrosis factor (TNF) production by mouse bone marrow-derived macrophages (BMDMs) exposed to wild-type or capsule-deficient (*cap60Δ*) *C. neoformans* (KN99α serotype A strain), the non-pathogen *Saccharomyces cerevisiae* (s288c), or the pathogen *Candida albicans* (SC5314). *C. neoformans* did not induce TNF, whereas *S. cerevisiae* and *C. albicans* both strongly induced TNF (Extended Data Fig. 1a). To investigate BMDM responses globally, we performed RNA sequencing (RNA-seq) on cells stimulated with lipopolysaccharide (LPS), zymosan (a product of *S. cerevisiae* cell walls), *S. cerevisiae*, and wild-type or capsule-deficient *C. neoformans*. *C. neoformans* induced negligible induction of inflammatory cytokine mRNAs (Extended Data Fig. 1c). Analysis of genes uniquely upregulated by *C. neoformans* revealed a partial signature reminiscent of alternatively activated or tolerized macrophages (M2 polarized macrophages), especially the

[1]Department of Biochemistry and Biophysics, University of California, San Francisco, CA, USA. [2]Department of Pharmaceutical Chemistry, University of California, San Francisco, CA, USA. [3]Cardiovascular Research Institute, University of California, San Francisco, CA, USA. [4]Chan–Zuckerberg Biohub, San Francisco, CA, USA. ✉e-mail: hitenmadhani@gmail.com

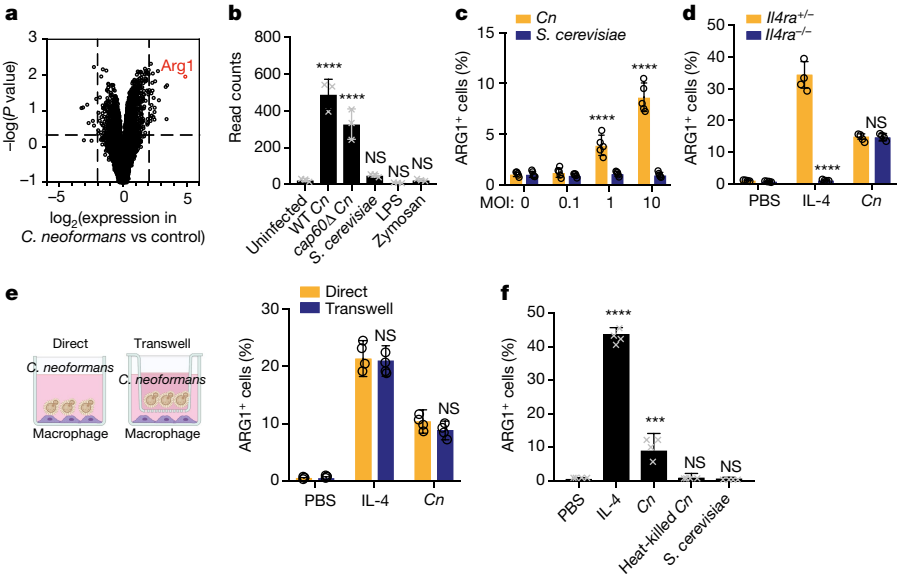

Fig. 1 | *Cryptococcus* promotes arginase-1 expression in macrophages via a soluble, capsule-independent mechanism. a, Volcano plot of RNA-seq data showing uniquely differentially expressed genes (filtered on genes with more than twofold change over *S. cerevisiae* challenge) between uninfected and 6 h wild-type *C. neoformans*-infected BMDMs based on DESeq2 analysis (multiplicity of infection (MOI) = 10). Three biological replicates were used for each condition. **b**, Normalized RNA-seq data for BMDMs stimulated for 6 h with either wild-type (WT) *C. neoformans* (*Cn*), *cap60Δ C. neoformans*, *S. cerevisiae* (all at MOI = 10), LPS (100 ng ml^{-1}), or zymosan (10 μg ml^{-1}). Three biological replicates were used for each condition. **c**, Intracellular fluorescence-activated cell sorting (FACS) detection of arginase-1 after 24 h of infection with either *C. neoformans* or *S. cerevisiae* at the indicated MOI. Five biologically independent samples. **d**, FACS detection of intracellular arginase-1 in *Il4ra*$^{+/-}$ and *Il4ra*$^{-/-}$ BMDMs stimulated for 24 h with IL-4 (40 ng ml^{-1}) or WT *C. neoformans* (MOI = 10). Four biologically independent samples. **e**, FACS detection of intracellular arginase-1 under identical conditions as in **d**, but with the stimuli either added directly to the BMDMs or to the top of a 0.2-μm Transwell insert (image created with BioRender.com). Four biologically independent samples. **f**, FACS detection of arginase-1 in BMDMs stimulated for 24 h with IL-4 (40 ng ml^{-1}), live wild-type *C. neoformans*, heat-killed (55 °C for 15 min) wild-type *C. neoformans* or *S. cerevisiae* (all MOI = 10). Four biologically independent samples. Data are mean ± s.d. ***$P < 0.001$, ****$P < 0.0001$ by one-way ANOVA with Bonferroni test.

induction of the M2 marker gene arginase-1 (*Arg1*), by both wild-type and capsule-deficient strains. (Fig. 1a and Extended Data Fig. 1d). There was minimal induction of *Arg1* by LPS, zymosan or *S. cerevisiae* (Fig. 1b and Extended Data Fig. 1d). These results suggested that *C. neoformans* harbours a capsule-independent immunomodulatory mechanism.

To verify this, we performed intracellular flow cytometry staining for arginase-1 and inducible nitric oxide synthase (iNOS) protein and confirmed specific upregulation by IL-4 and LPS, respectively (Extended Data Fig. 1e). *C. neoformans* induced arginase-1 protein in BMDMs, whereas no induction was observed with *S. cerevisiae* (Fig. 1c). Reciprocally, *Saccharomyces* drove high levels of iNOS, whereas minimal induction was seen after *C. neoformans* infection (Extended Data Fig. 1b). Type 2 cytokines such as IL-4 and IL-13 promote expression of ARG1 in macrophages; we thus tested whether *C. neoformans*-mediated ARG1 expression required IL-4Rα. However, *C. neoformans* induced similar levels of ARG1 in wild-type and *Il4ra*$^{-/-}$ BMDMs, suggesting an alternative mechanism (Fig. 1d). We found that the *C. neoformans*-derived signal was soluble and did not require direct cell–cell interactions, as the fungi could still promote arginase-1 expression across a 0.2 μm Transwell (Fig. 1e). However, heat-killed *C. neoformans* could not induce macrophage arginase-1, indicating that an active process is required (Fig. 1f).

Identification of a fungal effector

To understand how *C. neoformans* influences macrophage polarization, we performed a forward genetic screen using a *C. neoformans* knockout collection that we generated in the KN99α strain background. In this collection, most non-essential genes (n = 4,402) were individually replaced with a nourseothricin-resistance cassette (*NAT1*) by homologous recombination. We infected BMDMs with this collection in an arrayed format and then screened them by flow cytometry to identify *C. neoformans* mutant strains defective in macrophage arginase-1 induction (Fig. 2a). We re-screened the top 100 hits (Extended Data Fig. 2a) and identified 14 genes whose deletion yielded a reproducible defect in arginase-1 induction in response to *C. neoformans* (Extended Data Fig. 2b). Because we had already observed that the *C. neoformans*-derived signal was soluble, we focused on the one protein (encoded by *CNAG_02797/CPL1*) among the 14 gene products that harboured a predicted signal peptide. CPL1 is a predicted secreted protein of unknown molecular function with a cysteine-rich C-terminal domain (Fig. 2b). CPL1 was previously identified in an in vivo mouse screen of a small knockout library in a different yeast strain background and was found to have defects in fitness and in the production of visible polysaccharide capsule[21]. Another notable hit from our genetic screen was a knockout of *GAT201*, which encodes a transcription factor that is a key regulator of *C. neoformans* virulence, which binds to the *CPL1* promoter[21,22]. As effector proteins from plant fungal pathogens are highly enriched for small, secreted cysteine-rich proteins, we selected CPL1 for further study[23].

To complement the *cpl1*Δ phenotype, we inserted the *CPL1* gene into a neutral locus[24]. This complemented strain (*cpl1*Δ+*CPL1*) displayed restored arginase-1 induction capacity (Fig. 2c). In addition, overexpression of *CPL1* triggered increased arginase-1 induction (Fig. 2d). Experiments performed in different *C. neoformans* strain backgrounds have yielded different conclusions regarding the extent of the capsule defect of *cpl1*Δ mutants[25,26]. We found that, in the KN99α background used here, both India ink staining and FACS staining of yeast with antibodies against GXM—the major capsular polysaccharide—showed that the *cpl1Δ* strain contained equivalent to slightly increased surface GXM levels compared with wild type, whereas *cap60Δ* showed an expected loss of staining (Fig. 2e and Extended Data Fig. 2c). Although we did not expect capsule production to be related to the arginase-1 induction phenotype—as *cap60Δ* showed equivalent upregulation to wild type

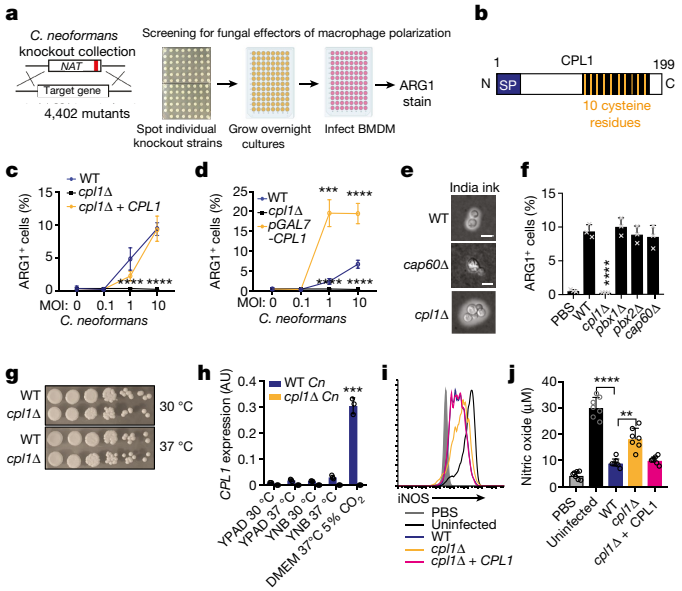

Fig. 2 | Identification of CPL1 as a fungal effector by forward genetics. **a**, Genetic screening strategy to identify fungal effectors that drive arginase-1 expression. **b**, Outline of CPL1 protein domain architecture. **c**, Complementation assay using FACS detection of arginase-1 in BMDMs stimulated for 24 h with either wild-type, *cpl1Δ* or *cpl1Δ* + CPL1 *C. neoformans* strains at the indicated MOI. Four biologically independent samples. **d**, FACS detection of arginase-1 in BMDMs stimulated for 24 h with wild-type, *cpl1Δ* or pGAL7-CPL1 *C. neoformans* strains at the indicated MOI. Four biologically independent samples. **e**, India ink staining for capsular polysaccharides in the indicated strains after overnight culture in 10% Sabouraud medium. Scale bar, 5 μm. Data are representative of two independent experiments. **f**, FACS detection of arginase-1 in BMDMs stimulated for 24 h with the indicated capsule mutant strains at MOI = 10. Three biologically independent samples. **g**, Spotting assay for wild-type versus *cpl1Δ C. neoformans* growth on YPAD plates incubated at the indicated temperatures. **h**, Quantitative PCR with reverse transcription (RT–qPCR) of *CPL1* mRNA in cultures grown to A_{600} of 1.0 in the indicated conditions. AU, arbitrary units relative to *ACT1*. Three biologically independent samples. **i**, Representative FACS detection of intracellular iNOS in BMDMs pre-infected with the indicated strains at MOI = 10 for 2 h followed by 24 h stimulation with LPS (100 ng ml^{-1}) and IFNγ (50 ng ml^{-1}). **j**, Total nitric oxide in supernatants from BMDMs treated as in **i**. Seven biologically independent samples. Data are mean ± s.d. $^{**}P < 0.01$, $^{***}P < 0.001$, $^{****}P < 0.0001$ by one-way ANOVA with Bonferroni test.

by RNA-seq and no classical capsule mutants were obtained in our screen—we nevertheless tested a series of capsule-related mutants that clustered with *cpl1Δ* in chemogenomic profiles[25]. None showed altered arginase-1 upregulation by BMDMs (Fig. 2f). Thus, the phenotype of *cpl1*Δ mutants on arginase-1 induction could not be explained by a defect in the capsule.

In addition to producing a capsule, *C. neoformans* has virulence attributes including the production of melanin, which is thought to have antioxidant properties, and the ability to grow[27] at 37 °C. We observed no specific defect for *cpl1*Δ in growth at 37 °C (Fig. 2g). We next tested whether temperature or culture conditions had any effect on *CPL1* expression, as genes related to virulence might be expected to show increased expression in mammalian tissue culture conditions. Indeed, we found that tissue culture conditions (37 °C, DMEM, 10% fetal calf serum and 5% CO_2) markedly increased CPL1 mRNA levels compared with culture in yeast peptone adenine dextrose (YPAD) or yeast nitrogen base (YNB) at either 30 °C or 37 °C (Fig. 2h). The upregulation of *CPL1* in mammalian tissue culture conditions involved redundant contributions of 5% CO_2 and 10% fetal calf serum (Extended Data Fig. 2d). We found qualitatively equivalent melanin induction (Extended Data Fig. 2e). Finally, we examined macrophage TNF production in response to challenge with *cpl1Δ C. neoformans* to determine whether the loss of arginase-1 expression was secondary to a gain in classical macrophage activation. Whereas zymosan generated a strong response from BMDMs, neither wild-type nor *cpl1Δ C. neoformans* elicited any TNF production (Extended Data Fig. 2f).

C. neoformans can suppress nitric oxide production by macrophages in response to LPS and IFNγ via a capsule-independent mechanism[27]. As alternative macrophage activation antagonizes the induction of antimicrobial factors such as iNOS, we tested whether *CPL1* had an effect on iNOS expression and nitric oxide production. We infected BMDMs for 2 h with either wild-type, *cpl1*Δ or *cpl1*Δ+*CPL1 C. neoformans* followed by stimulation with LPS and IFNγ for 24 h. We then used flow cytometry to assess iNOS expression and quantified total nitric oxide in the BMDM supernatants. Consistent with previous reports, we found that wild-type *C. neoformans* suppressed iNOS expression and nitric oxide production (Fig. 2i,j). Notably, the *cpl1*Δ strain was defective in suppressing iNOS expression and nitric oxide production (Fig. 2i,j). This effect was potent but not complete, indicating that additional modulators exist.

Fungal potentiation of IL-4 signalling

We hypothesized that CPL1 might act directly on macrophages. To test this model, we expressed recombinant CPL1–His_6 (rCPL1) using the yeast *Pichia pastoris* (Fig. 3a). We stimulated macrophages with dilutions of purified protein, or the equivalent dilutions derived from mock purifications from wild-type yeast to control for potential background contaminants. Using flow cytometry, we found that rCPL1 could induce arginase-1 in BMDMs at nanomolar concentrations (Fig. 3b). Using a strain with an endogenous allele encoding CPL1–His_6, we found that the endogenous concentration of this protein produced in supernatants under mammalian tissue culture conditions was around 10 nM, which was within the range in which we observe activity (Extended Data Fig. 3a). As *C. neoformans* is known to induce type 2 cytokines such as IL-4 during pulmonary infection, we tested whether rCPL1 induction of arginase-1, a well-known IL-4-responsive gene, might reflect an ability to enhance the effects of IL-4. We stimulated BMDMs with IL-4 along with dilutions of rCPL1. We found that rCPL1 potentiated the induction of arginase-1 by IL-4 (Fig. 3b). We additionally observed that wild-type *C. neoformans* strongly potentiated induction of *Arg1* mRNA in BMDMs by IL-4 in a *CPL1*-dependent manner (Extended Data Fig. 3b). Although ARG1 is not a marker of human IL-4-stimulated myeloid cells, we found that *Mrc1* mRNA expression could be potentiated by *C. neoformans* in the THP-1 human monocytic cell line as well as in primary human monocyte-derived macrophages (Extended Data Fig. 3c,d).

RNA-seq analysis of BMDMs stimulated for 24 h with either PBS, IL-4 alone, rCPL1 alone or both IL-4 and rCPL1 confirmed that rCPL1 increased expression of a large subset of IL-4-induced genes, indicating that this effect is not specific to ARG1 expression (Fig. 3c and Extended Data Fig. 3e). The RNA-seq data also showed marked potentiation of IL-4-induced *Arg1* mRNA expression by rCPL1 (Extended Data Fig. 3e). Another gene that showed strong expression potentiation by rCPL1 and IL-4 was *Ccl24*, which encodes an eosinophil chemoattractant (Extended Data Fig. 3e). Using a Transwell migration assay, we found that splenic eosinophils indeed showed increased chemotaxis towards supernatants derived from BMDMs stimulated with IL-4 and rCPL1 compared to those stimulated with IL-4 alone (Extended Data Fig. 3f). *C. neoformans* also showed enhanced growth in supernatants from BMDMs stimulated with IL-4 and rCPL1 compared to supernatants treated with either IL-4 or rCPL1 alone, suggesting that alternatively activated macrophages may secrete nutrients that promote fungal growth (Fig. 3d). These results demonstrated that CPL1 enhances the effect of IL-4 on macrophages, generating conditions that are beneficial to fungal growth in vitro.

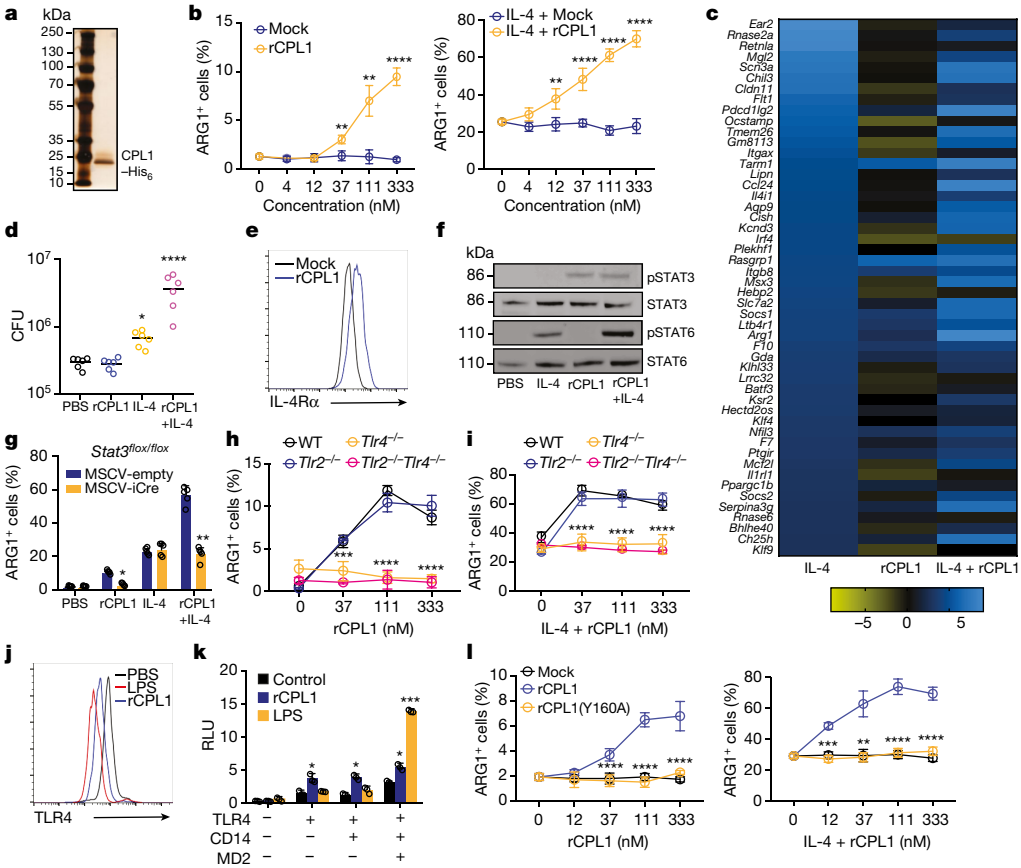

Fig. 3 | CPL1 potentiates IL-4 signalling via TLR4. a, Silver-stained SDS–PAGE of recombinant CPL1. $n = 5$ independent experiments. **b**, FACS detection of arginase-1 in BMDMs stimulated for 24 h with mock or purified rCPL1 alone (left) or with IL-4 (right). Three biologically independent samples. **c**, RNA-seq heat map of the top 50 BMDM IL-4-induced genes comparing the fold changes of the indicated stimulations relative to PBS. **d**, No of *C. neoformans* after 48 h of incubation at 37 °C and 5% CO_2 in supernatants from BMDMs stimulated for 24 h as in **c**. CFU, colony-forming units. Six biologically independent samples. **e**, FACS detection of IL-4Rα on BMDMs stimulated for 24 h with rCPL1 or mock. **f**, Western blot for indicated proteins in BMDMs stimulated as in **c** for 8 h. Data are representative of three independent experiments. **g**, FACS detection of arginase-1 in *STAT3*$^{flox/flox}$ BMDMs transduced with empty vector or iCre retrovirus and stimulated as in **c**. Five biologically independent samples. **h**, FACS detection of arginase-1 in wild-type, *Tlr2*$^{-/-}$, *Tlr4*$^{-/-}$ or *Tlr2*$^{-/-}$*Tlr4*$^{-/-}$ BMDMs stimulated for 24 h with rCPL1. Three biologically independent samples. **i**, As **h** but with IL-4 stimulation. Three biologically independent samples. **j**, FACS detection of TLR4 on BMDMs stimulated for 1 h with LPS (100 ng ml^{-1}) or rCPL1. Three biological experiments. **k**, Luminescence in HEK293T cells transfected with the indicated plasmids plus NF-kB luciferase and stimulated for 6 h with either rCPL1 or LPS (100 ng ml^{-1}). Three biologically independent samples. **l**, FACS detection of arginase-1 in BMDMs stimulated for 24 h with mock, rCPL1 or rCPL1(Y160A) alone (left) or in combination with IL-4 (right). Three biologically independent samples. Concentrations are 10 ng ml^{-1} for IL-4 and 111 nM for rCPL1 unless otherwise noted. Data are mean ± s.d. $^*P < 0.05$, $^{**}P < 0.01$, $^{***}P < 0.001$, $^{****}P < 0.0001$ by one-way ANOVA with Bonferroni test.

We investigated how CPL1 and IL-4 may cooperate to amplify the IL-4 transcriptional signature. One hypothesis was that CPL1 may enhance macrophage sensitivity to IL-4 at the level of the receptor's expression. Indeed, FACS staining revealed that *C. neoformans* drove increased surface levels of BMDM IL-4Rα in a manner dependent on *CPL1*, and that rCPL1 was sufficient to produce this effect (Fig. 3e and Extended Data Fig. 4a). *Salmonella typhimurium* has been reported to drive macrophage M2-like polarization via the effector protein SteE, which activates phosphorylation of STAT3[28,29] (pSTAT3). We noted that the readout for M2 polarization in those reports was increased IL-4Rα levels, and that STAT3 was required for IL-4Rα upregulation by *Salmonella*. To test whether similar signalling pathways were required for the activity of CPL1, we performed western blots on extracts of BMDMs to assess phosphorylation of STAT3 and STAT6 (pSTAT6) after stimulation with either IL-4, rCPL1, or IL-4 plus rCPL1. Whereas we saw no effect of CPL1 during immediate early time points (Extended Data Fig. 4b,c and Supplementary Figure 1), at 8 h after stimulation rCPL1 drove hyper-phosphorylation of STAT6 when given in combination with IL-4 (Fig. 3f, Extended Data Fig. 4d and Supplementary Figure 1). Time-course analysis showed that rCPL1 promoted STAT3 phosphorylation starting at 2 h after stimulation in BMDMs, consistent with STAT3 activation preceding hyper-STAT6 activation (Extended Data Fig. 4e). To test the requirement for STAT3, we transduced *Stat3*$^{flox/flox}$ bone marrow using murine retrovirus (MSCV) encoding iCre and generated BMDMs. STAT3 was found to be required for both arginase-1 induction and IL-4 potentiation by CPL1 (Fig. 3g). These data indicate that activation of STAT3 is downstream of CPL1.

TLR4 as a mediator of CPL1 activity

We next sought to identify receptors involved in this process. Previous work had shown that Bacillus Calmette Guerrin (BCG) can thwart macrophage intracellular immunity by promoting expression of arginase-1[30] via engagement of TLR2-MyD88 signalling to activate STAT3, which drives transcription of arginase-1. We therefore tested *MyD88*$^{-/-}$ BMDMs in our arginase-1 assays. We found that MyD88 deficiency abrogated arginase-1 upregulation by rCPL1 (Extended Data Fig. 5a). We also observed that rCPL1 instead quenched arginase-1 upregulation by IL-4 in *MyD88*$^{-/-}$ BMDMs, which may be owing to the induction of type I IFN downstream via the adaptor TRIF (Extended Data Fig. 5a). We

hypothesized that MyD88 signalling promoted STAT3 phosphorylation via induction of autocrine- or paracrine-acting cytokines. As predicted by such a model, we found that co-culture of CD45.2$^+$ *MyD88*$^{-/-}$ BMDMs with wild-type congenic (CD45.1$^+$) BMDMs rescued the arginase-1 induction (Extended Data Fig. 5b).

As MyD88 is an adaptor molecule for Toll-like receptor (TLR) signalling[31], we tested whether TLRs were required for the activity of CPL1. We found that deletion of *Unc93b1*, which is required for endosomal nucleic acid-sensing TLRs to function[32], did not affect CPL1-dependent arginase-1 induction (data not shown). However, we found abrogation of arginase-1 induction in response to CPL1 in the absence of the LPS receptor TLR4, whereas TLR2 deficiency had no effect (Fig. 3h,i). There are molecules, such as palmitic acid, that activate TLR4 signalling without directly binding the receptor[33]. Notably, whereas TLR4-binding agonists direct rapid TLR4 endocytosis[34], indirect activators such as palmitic acid do not result in TLR4 internalization[33]. To test the effect of CPL1 in TLR internalization, we stained BMDMs stimulated for 1 h with either LPS or rCPL1 and measured TLR4 surface levels by flow cytometry. We found that rCPL1 stimulation decreased surface TLR4 levels (Fig. 3j), but not to the same extent as LPS, consistent with a model in which CPL1 is a TLR4 ligand.

Although our data did not find robust arginase-1 induction by LPS, we nonetheless addressed whether CPL1 phenotypes could be a result of LPS contamination. First, we stimulated BMDMs with dilutions of LPS and tested arginase-1 upregulation. We found that LPS only induced robust arginase-1 at a high concentration (1 μg ml^{-1}) (Extended Data Fig. 5c). As the high amount of LPS required for arginase-1 upregulation was at a concentration that induced robust caspase-11-dependent pyroptosis when given with cholera toxin B (CTB) (Extended Data Fig. 5d), we reasoned that if the effect of CPL1 were due to LPS contamination, we would observe pyroptosis when stimulating BMDMs with CPL1 and CTB[35,36]. However, we observed no pyroptosis induced by stimulation with CPL1 and CTB (Extended Data Fig. 5e). LPS is heat stable, whereas proteins can be denatured by heat. We observed that boiling of rCPL1 completely abrogated arginase-1 induction and potentiation by IL-4, again consistent with a role for CPL1 protein and not LPS (Extended Data Fig. 5f). As another approach, we incubated rCPL1 with polymyxin B to sequester any LPS in the preparation. We found that polymyxin B treatment had no effect on the ability of rCPL1 to promote arginase-1 expression (Extended Data Fig. 5g,h). Finally, we tested whether expression of CPL1 in BMDMs could phenocopy the effect of the purified recombinant protein, as this would prevent the possibility of introducing microbial contaminants. We cloned CPL1 into a mouse retroviral vector with an IL-2 signal peptide and transduced mouse bone marrow. After differentiation into BMDMs, we stimulated these cells with dilutions of IL-4. We found that transduction of CPL1 into macrophages potentiated the IL-4 induction of arginase-1 compared with control transductions (Extended Data Fig. 5i). Together, these data strongly support the conclusions that CPL1 activates TLR4 and that this is not owing to inadvertent endotoxin contamination.

Although it is best known as a sensor of LPS, TLR4 has a key role in driving allergic inflammation in response to house dust mite extract (HDM), and low doses of LPS can also drive allergic inflammation in response to ovalbumin[10,11]. Two dominant allergens in HDM are the protease Derp1 and the lipid-binding protein Derp2[37,38]. One mechanism by which Derp2 drives allergic responses is by acting as an MD2 mimic to activate TLR4[9]. To test whether CPL1 could activate TLR4 via a similar mechanism, we reconstituted NF-kB–luciferase reporter expressing HEK293T cells with mouse TLR4 alone or in combination with co-receptors CD14 and MD2 and then stimulated these cells with rCPL1 or LPS. Whereas LPS drove luciferase expression only when TLR4 was co-expressed with CD14 and MD2, rCPL1 induced luciferase in cells expressing TLR4 only, suggesting that CPL1 can bypass a requirement for MD2 in TLR4 activation (Fig. 3k). In previous studies on Derp2, it was found that mutation of a key tyrosine residue flanked by two cysteines, which is similar to a conserved motif found on MD2, abrogated TLR4 activation, despite no sequence homology between the two proteins[9]. We analysed the CPL1 amino acid sequence and generated a recombinant protein with a mutation (Y160A) in an analogous motif (Extended Data Fig. 5j). This mutation eliminated the ability of CPL1 to augment both IL-4-independent and IL-4-dependent arginase-1 expression (Fig. 3l). Although it remains to be demonstrated whether CPL1 indeed activates TLR4 via an analogous mechanism to that of Derp2, this result provided an additional control for possible contaminants.

Finally, to control for effects that may be specific to proteins from *P. pastoris*, we purified CPL1 from supernatants of a *C. neoformans* strain expressing CPL1–His_6 under the control of the H3 promoter and inserted into a neutral locus. We found that this rCPL1 also promotes arginase-1 on its own and potentiates IL-4-induced arginase-1 expression in BMDMs in a TLR4-dependent manner (Extended Data Fig. 6a,b).

CPL1 enhances type 2 immunity in vivo

We next examined whether CPL1 contributes to type 2 inflammation during in vivo pulmonary infection. Deletion of IL-4 signalling in myeloid cells has been shown to be beneficial to the host during *Cryptococcus* infection; however, the lung myeloid compartment is highly heterogenous and the specific identity of the arginase-1-expressing cells during fungal infection remains unclear[4,39]. We infected arginase-1–YFP reporter (YARG) mice with wild-type *C. neoformans* and processed lung tissue for flow cytometry on day 10 after infection. Analysis of the CD45$^+$YARG$^+$ cells revealed that interstitial macrophages (CD45$^+$CD64$^+$MerTK$^+$SiglecF$^-$) are the major cell type that expresses ARG1 during infection (Fig. 4a,b). To test the role of CPL1, we infected YARG mice intranasally with either wild-type, *cpl1Δ* or *qsp1Δ C. neoformans* (*qsp1Δ* lacks a secreted peptide that is important during in vivo infection[22]). We found that *cpl1Δ* infection resulted in a striking reduction in YARG$^+$ interstitial macrophages compared with both wild-type and *qsp1Δ* infections (Fig. 4c). To determine whether this decrease in YARG+ cells was secondary to a global reduction in type 2 immunity we assessed other outputs of IL-4 and IL-13 signalling, such as eosinophilia, IgG1 class switching in germinal centre B cells and cytokine production by CD4$^+$ T cells. Compared with infection with wild-type or *qsp1Δ*, *cpl1Δ C. neoformans* infection showed a modest reduction in lung eosinophils (Extended Data Fig. 7a), which is not surprising given that IL-4-stimulated macrophages produce eosinophil-recruiting chemokines such as CCL24[40]. By contrast, we observed no difference between the fungal genotypes in the levels of IL-4-dependent IgG1 class switching (Extended Data Fig. 7b,c) or in CD4+ T cell cytokine production (Extended Data Fig. 7d,e). These data identify a crucial role for CPL1 in promoting local type 2 inflammation in the lung, although we cannot rule out effects on additional cell types beyond interstitial macrophages.

A defect in type 2 cytokine signalling increases the survival of mice infected with *C. neoformans*[4,8,17]. Since we found that mice infected with *cpl1Δ C. neoformans* exhibited decreased type 2 inflammation, we tested whether *CPL1* impacted mouse survival. Of note, we found that nearly all mice survived infection by a strain lacking *CPL1* (Fig. 4d). Complementation of the mutant with the wild-type gene rescued the in vivo YARG and eosinophil defects as well as the virulence defect (Extended Data Fig. 8a–c). Infection with *cpl1Δ C. neoformans* additionally resulted in decreased fungal burden in the brain (Extended Data Fig. 8d). We confirmed that YARG induction in response to *C. neoformans* infection was indeed dependent on type 2 cytokine signalling using both IL-4Rα- and STAT6-deficient mice (Fig. 4e).

As CPL1 may have contributions to virulence in vivo beyond augmentation of type 2 inflammation, we tested whether the *cpl1Δ* mutant displayed phenotypes in mice lacking factors critical for type 2 responses. We infected wild-type, *Il4ra*$^{-/-}$ and *Stat6*$^{-/-}$ mice with either wild-type or *cpl1Δ C. neoformans* and then measured the titre of *C. neoformans* in the lung on day 10. Consistent with previous reports, we found that

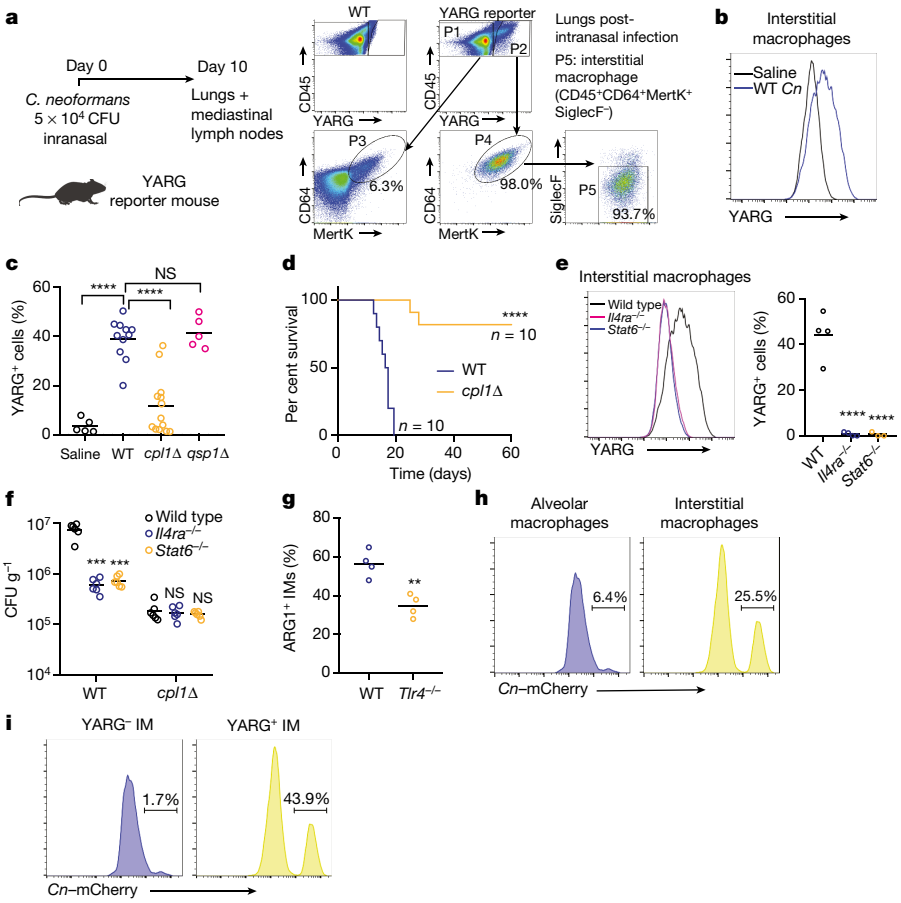

Fig. 4 | CPL1 promotes arginase-1 expression in pulmonary interstitial macrophages and is required for virulence. a, FACS sub-gating of CD45⁺YARG⁺ lung cells from YARG mice infected intranasally with 5×10^4 CFU wild-type *C. neoformans* for 10 days. **b**, Representative histogram of YARG expression in lung interstitial macrophages from mice injected intranasally with either saline or 5×10^4 CFU wild-type *C. neoformans* for 10 days. **c**, FACS detection of YARG expression in interstitial macrophages from mice injected intranasally with either saline ($n = 5$ mice), or wild-type ($n = 11$ mice), *cpl1Δ* ($n = 14$ mice) or *qsp1Δ* ($n = 5$ mice) Kn99a (5×10^4 CFU) for 10 days. One-way ANOVA with Bonferroni test. **d**, Kaplan–Meier survival curve analysis of mice infected with wild-type ($n = 10$ mice) or *cpl1Δ* ($n = 10$ mice) *C. neoformans*. ****$P < 0.0001$ by Mantel–Cox test. **e**, Representative histogram (left) and quantification (right) showing YARG expression in WT, *Il4ra*$^{-/-}$ or *Stat6*$^{-/-}$ (all $n = 4$ mice) infected for 10 days as in **a**. **f**, Lung titre of wild-type and *cpl1Δ* *C. neoformans* in the indicated mouse genotypes ($n = 6$ mice for each genotype) 10 days after infection. One-way ANOVA with Bonferroni test. **g**, FACS detection of arginase-1 in lung interstitial macrophages (IMs) from WT or *Tlr4*$^{-/-}$ mice infected as in **a**. Unpaired two-sided *t*-test. **h**, Representative FACS detection of *C. neoformans*–mCherry expression in alveolar macrophages (left) or interstitial macrophages (right) after 10 days of infection. **i**, Representative FACS histograms of *C. neoformans*–mCherry expression in interstitial macrophages from YARG mice gated on YARG⁻ interstitial macrophages (left) or YARG⁺ interstitial macrophages (right). *$P < 0.05$, **$P < 0.01$, ***$P < 0.001$, ****$P < 0.0001$.

IL-4Rα- and STAT6-deficient mice showed lower pulmonary fungal burden than wild-type mice (Fig. 4f). However, whereas *cpl1Δ* infections showed decreased numbers of colony-forming units relative to the control strain in wild-type mice, there was no further decrease in IL-4Rα- and STAT6-deficient hosts (Fig. 4f). This result suggests that induction of type 2 inflammation is required for CPL1 to affect infectivity. We reasoned that simultaneous infection of mice with wild-type *C. neoformans* might rescue *cpl1Δ C. neoformans* via the induction of type 2 immunity in *trans*. We performed mixed intranasal infections (WT versus WT with kanamycin resistance (KanR), *cpl1Δ* versus *cpl1Δ* (KanR) and WT (KanR) versus *cpl1Δ*) using congenic G418-resistant mixing partners and found that co-infection with wild type partially restored the number of pulmonary *cpl1Δ C. neoformans* (Extended Data Fig. 8e). Although there are likely to be additional mechanisms by which CPL1 promotes *C. neoformans* pathogenesis, these data indicate that promotion of type 2 immunity is a critical function of this virulence factor.

Since BMDM polarization by CPL1 requires TLR4, we tested whether TLR4 contributed to type 2 inflammation in response to pulmonary infection. We found that *Tlr4*$^{-/-}$ mice infected with *C. neoformans* displayed reduced arginase-1 expression in interstitial macrophages as well as reduced pulmonary fungal burden and eosinophilia (Fig. 4g and Extended Data Fig. 9a,b). To investigate the role of CPL1 in animals but in the absence of pathogen–host dynamics, we tested whether rCPL1 protein alone could drive type 2 inflammation. We challenged wild-type and *Tlr4*$^{-/-}$ mice intranasally with different doses of CPL1 and then assessed pulmonary eosinophilia on day 21. Intranasal treatment of mice with rCPL1 (but not with bovine serum albumin) was sufficient to induce pulmonary eosinophilia; this induction was fully dependent on TLR4 (Extended Data Fig. 9c).

Alternatively, activated macrophages can be exploited as a replicative niche by pathogens owing to their reduced ability to kill microbes[41]. To begin to test this hypothesis, we performed flow cytometric analysis of pulmonary tissue from YARG mice infected intranasally with mCherry-expressing *C. neoformans*. We observed high mCherry⁺ signal associated with interstitial macrophages compared with alveolar macrophages (Fig. 4h). Sub-gating interstitial macrophages into either YARG⁻ or YARG⁺ populations further showed a substantial enrichment of mCherry⁺ *C. neoformans* in the YARG⁺ cells (Fig. 4i). These data demonstrate a selective association of *C. neoformans* with arginase-expressing interstitial macrophages in vivo.

Discussion

We identified CPL1 as a secreted effector of *C. neoformans* that promotes fungal virulence by enhancing type 2 inflammation. Our work supports a model in which CPL1 activates TLR4 signalling to drive phosphorylation of STAT3 in macrophages, which both promotes the initial induction of arginase-1 and amplifies macrophage sensitivity to IL-4 signalling (Extended Data Fig. 9d). In vivo, CPL1 is required for virulence and promotes the induction of arginase-1 by interstitial macrophages. *C. neoformans* also physically associates with polarized interstitial macrophages during infection, consistent with direct macrophage reprogramming in vivo by CPL1. Future detailed biochemical and structural studies will be required understand the precise mechanism of TLR4 activation by CPL1, which could involve the modulation of canonical as well as noncanonical co-receptors and/or signalling mechanisms.

Online content

Any methods, additional references, Nature Research reporting summaries, source data, extended data, supplementary information, acknowledgements, peer review information; details of author contributions and competing interests; and statements of data and code availability are available at https://doi.org/10.1038/s41586-022-05005-4.

1. Armstrong-James, D., Meintjes, G. & Brown, G. D. A neglected epidemic: fungal infections in HIV/AIDS. *Trends Microbiol.* **22**, 120–127 (2014).
2. Brown, G. D. et al. Hidden killers: human fungal infections. *Sci. Transl. Med.* **4**, 165rv13 (2012).
3. Zhao, Y., Lin, J., Fan, Y. & Lin, X. Life cycle of *Cryptococcus neoformans*. *Annu. Rev. Microbiol.* **73**, 17–42 (2019).
4. Müller, U. et al. Abrogation of IL-4 receptor-α-dependent alternatively activated macrophages is sufficient to confer resistance against pulmonary cryptococcosis despite an ongoing T_h2 response. *Int. Immunol.* **25**, 459–470 (2013).
5. Mueller, U. et al. IL-13 induces disease-promoting type 2 cytokines, alternatively activated macrophages and allergic inflammation during pulmonary infection of mice with *Cryptococcus neoformans*. *J. Immunol.* **179**, 5367–5377 (2007).
6. Wiesner, D. L. et al. Chitin recognition via chitotriosidase promotes pathologic type-2 helper T cell responses to cryptococcal infection. *PLoS Pathog.* **11**, e1004701 (2015).
7. Schulze, B. et al. $CD4^+FoxP3^+$ regulatory T cells suppress fatal T helper 2 cell immunity during pulmonary fungal infection. *Eur. J. Immunol.* **44**, 3596–3604 (2014).
8. Stenzel, W. et al. IL-4/IL-13-dependent alternative activation of macrophages but not microglial cells is associated with uncontrolled cerebral cryptococcosis. *Am. J. Pathol.* **174**, 486–496 (2009).
9. Trompette, A. et al. Allergenicity resulting from functional mimicry of a Toll-like receptor complex protein. *Nature* **457**, 585–588 (2009).
10. Hammad, H. et al. House dust mite allergen induces asthma via Toll-like receptor 4 triggering of airway structural cells. *Nat. Med.* **15**, 410–416 (2009).
11. Eisenbarth, S. C. et al. Lipopolysaccharide-enhanced, toll-like receptor 4-dependent T helper cell type 2 responses to inhaled antigen. *J. Exp. Med.* **196**, 1645–1651 (2002).
12. Millien, V. O. et al. Cleavage of fibrinogen by proteinases elicits allergic responses through Toll-like receptor 4. *Science* **341**, 792–796 (2013).
13. Ademe, M. & Girma, F. *Candida auris*: from multidrug resistance to pan-resistant strains. *Infect. Drug Resist.* **13**, 1287–1294 (2020).
14. Wall, G. & Lopez-Ribot, J. L. Current antimycotics, new prospects, and future approaches to antifungal therapy. *Antibiotics* **9**, 445 (2020).
15. Selin, C., de Kievit, T. R., Belmonte, M. F. & Fernando, W. G. D. Elucidating the role of effectors in plant-fungal interactions: progress and challenges. *Front. Microbiol.* **7**, 600 (2016).
16. Rajasingham, R. et al. Global burden of disease of HIV-associated cryptococcal meningitis: an updated analysis. *Lancet Infect. Dis.* **17**, 873–881 (2017).
17. Mueller, U. et al. Lack of IL-4 receptor expression on T helper cells reduces T helper 2 cell polyfunctionality and confers resistance in allergic bronchopulmonary mycosis. *Mucosal Immunol.* **5**, 299–310 (2012).
18. Kindermann, M. et al. Group 2 innate lymphoid cells (ILC2) suppress beneficial type 1 immune responses during pulmonary cryptococcosis. *Front. Immunol.* **11**, 209 (2020).
19. May, R. C., Stone, N. R. H., Wiesner, D. L., Bicanic, T. & Nielsen, K. *Cryptococcus*: from environmental saprophyte to global pathogen. *Nat. Rev. Microbiol.* **14**, 106–117 (2016).
20. Vecchiarelli, A. Immunoregulation by capsular components of *Cryptococcus neoformans*. *Med. Mycol.* **38**, 407–417 (2000).
21. Liu, O. W. et al. Systematic genetic analysis of virulence in the human fungal pathogen *Cryptococcus neoformans*. *Cell* **135**, 174–188 (2008).
22. Homer, C. M. et al. Intracellular action of a secreted peptide required for fungal virulence. *Cell Host Microbe* **19**, 849–864 (2016).
23. Stergiopoulos, I. & de Wit, P. J. G. M. Fungal effector proteins. *Annu. Rev. Phytopathol.* **47**, 233–263 (2009).
24. Arras, S. D. M., Chitty, J. L., Blake, K. L., Schulz, B. L. & Fraser, J. A. A genomic safe haven for mutant complementation in *Cryptococcus neoformans*. *PLoS ONE* **10**, e0122916 (2015).
25. Brown, J. C. S. et al. Unraveling the biology of a fungal meningitis pathogen using chemical genetics. *Cell* **159**, 1168–1187 (2014).
26. Kumar, P. et al. Pbx proteins in *Cryptococcus neoformans* cell wall remodeling and capsule assembly. *Eukaryot. Cell* **13**, 560–571 (2014).
27. Kawakami, K., Zhang, T., Qureshi, M. H. & Saito, A. *Cryptococcus neoformans* inhibits nitric oxide production by murine peritoneal macrophages stimulated with interferon-gamma and lipopolysaccharide. *Cell. Immunol.* **180**, 47–54 (1997).
28. Gibbs, K. D. et al. The *Salmonella* secreted effector SarA/SteE mimics cytokine receptor signaling to activate STAT3. *Cell Host Microbe* **27**, 129–139.e4 (2020).
29. Panagi, I. et al. *Salmonella* effector SteE converts the mammalian serine/threonine kinase GSK3 into a tyrosine kinase to direct macrophage polarization. *Cell Host Microbe* **27**, 41–53.e6 (2020).
30. Kasmi, El,K. C. et al. Toll-like receptor-induced arginase 1 in macrophages thwarts effective immunity against intracellular pathogens. *Nat. Immunol.* **9**, 1399–1406 (2008).
31. Deguine, J. & Barton, G. M. MyD88: a central player in innate immune signaling. *F1000Prime Rep.* **6**, 97 (2014).
32. Lind, N. A., Rael, V., Pestal, K., Liu, B. & Barton, G. M. Regulation of the nucleic acid-sensing Toll-like receptors. *Nat. Rev. Immunol.* **22**, 224–235 (2022).
33. Lancaster, G. I. et al. Evidence that TLR4 is not a receptor for saturated fatty acids but mediates lipid-induced inflammation by reprogramming macrophage metabolism. *Cell Metab.* **27**, 1096–1110.e5 (2018).
34. Zanoni, I. et al. CD14 controls the LPS-induced endocytosis of Toll-like receptor 4. *Cell* **147**, 868–880 (2011).
35. Hagar, J. A., Powell, D. A., Aachoui, Y., Ernst, R. K. & Miao, E. A. Cytoplasmic LPS activates caspase-11: implications in TLR4-independent endotoxic shock. *Science* **341**, 1250–1253 (2013).
36. Kayagaki, N. et al. Noncanonical inflammasome activation by intracellular LPS independent of TLR4. *Science* **341**, 1246–1249 (2013).
37. Chevigné, A. & Jacquet, A. Emerging roles of the protease allergen Derp1 in house dust mite-induced airway inflammation. *J. Allergy Clin. Immunol.* **142**, 398–400 (2018).
38. Jacquet, A. Characterization of innate immune responses to house dust mite allergens: pitfalls and limitations. *Front. Allergy* **2**, 662378 (2021).
39. Evren, E., Ringqvist, E. & Willinger, T. Origin and ontogeny of lung macrophages: from mice to humans. *Immunology* **160**, 126–138 (2020).
40. Makita, N., Hizukuri, Y., Yamashiro, K., Murakawa, M. & Hayashi, Y. IL-10 enhances the phenotype of M2 macrophages induced by IL-4 and confers the ability to increase eosinophil migration. *Int. Immunol.* **27**, 131–141 (2015).
41. Price, J. V. & Vance, R. E. The macrophage paradox. *Immunity* **41**, 685–693 (2014).

Methods

Mice

Wild-type C57BL/6J mice were purchased from Jackson Laboratories and bred in house. *MyD88*$^{-/-}$, *Tlr4*$^{-/-}$ and *Stat3*$^{flox/flox}$ mice were purchased from Jackson Laboratories. YARG reporter, *Il4ra*$^{-/-}$ and *Stat6*$^{-/-}$ mice were a gift from R. Locksley. BoyJ (B6.SJL-*Ptprc*^{a}*Pepc*^{b}/BoyJ) mice were a gift from J. Cyster. Animals were housed in a specific-pathogen free environment in the Laboratory Animal Research Center at UCSF. All experiments conformed to ethics and guidelines approved by the UCSF Institutional and Animal Care and Use Committee.

Yeast manipulations

Yeast genetic manipulations were performed as previously described[42]. Insertion of genes was obtained through homologous recombination by transforming 10 μg of digested plasmid.

Intranasal infections

Individual colonies from *Cryptococcus* plates were cultured overnight in 10 ml YPAD at 30 °C. The next day, yeast were counted on a haemocytometer and diluted to 1×10^6 cells per ml in saline. Mice were anaesthetized with intraperitoneal ketamine/dexmedetomidine and then hung by their front teeth using surgical thread. 50 μl yeast (5×10^4 CFU) were then pipetted onto the nasal flares and taken up by aspiration. For survival curves, the mice were weighed and assessed for clinical endpoints every 2 days for the first week post-infection, and then every day starting after week 1.

Intranasal injection of CPL1

Mice were anaesthetized with intraperitoneal ketamine/dexmedetomidine and then hung by their front teeth using surgical thread for intranasal injection. Mice were injected with 100 ng of either bovine serum albumin (Sigma) or recombinant CPL1 on day 0, 1 and 2, injected with 25 ng of either protein on days 14, 15, 17, 18 and 19 and then euthanized for analysis on day 21.

Generation of BMDMs

On day 0, mice were euthanized and femurs and tibias were collected into RPMI (2% FCS). The ends of the bones were clipped with scissors, and then bone marrow was flushed using a 25.5 gauge syringe. The bone marrow was then suspended in complete DMEM (10% FCS, HEPES, glutamine, penicillin/streptomycin) and 10% mCSF medium derived from 3T3-mCSF cells. Bone marrow suspensions were plated in non-tissue culture-treated 10 cm petri dishes. On day 4, 3 ml of additional 10% mCSF medium was added to each plate. The adherent macrophages were then collected on day 6 and either plated out for experiments or frozen.

Generation of human monocyte-derived macrophages

On day 0, monocytes were enriched from donated human peripheral blood mononuclear cells through successive Ficoll (Sigma Aldrich) and Percoll (GE Healthcare) gradients. Monocytes were then allowed to adhere to non-tissue culture-treated bacterial petri dishes for 1 h at 37 °C. Cells were then cultured for 7 days in IMDM + 10% AB human serum (Life Technologies). On day 7, cells were lifted from the plates using 0.05% Trypsin-EDTA, and seeded onto 24-well TC-treated plates at 500,000 cells per well. Human monocyte-derived macrophages were then stimulated for 24 h with recombinant human IL-4 (Peprotech) and the indicated fungal strains.

Retroviral transduction of BMDMs

On day 0, bone marrow was collected and cultured in 10% mCSF medium as above and mouse retroviral MSCV plasmid encoding CPL1 or iCre was transfected into platE cells using Lipofectamine 2000 (Thermo Fisher Scientific). On day 2, viral supernatants were collected and filtered through a 0.45-μm syringe filter. Non-adherent bone marrow cells were collected and spun down in 6-well plates. The supernatant was aspirated, and 2 ml of retrovirus was added to each well along with 10 μg ml^{-1} Polybrene (Sigma). The plates were then spun for 2 h at room temperature at 2,400 rpm with no brake. After spinning, the retroviral supernatants were aspirated and replaced with 10% mCSF medium. On day 3, another round of identical spinfection was performed. Cells were then collected for experiments on day 6.

ELISA

High-binding half-area 96-well plates (Corning) were coated with 25 μl of unconjugated anti-TNF antibody (Invitrogen; clone 1F3F3D4) at a concentration of 2 μg ml^{-1} in PBS and incubated overnight at 4 °C. Plates were then washed 6 times with PBST (1× PBS + 0.05% Tween-20) and blocked for 1 h at room temperature with 120 μl of 1× PBS + 5% FCS. Next, the blocking solution was removed and 25 μl of indicated macrophages supernatants plus a standard curve using recombinant mouse TNF (Peprotech) in 1× PBS + 5% FCS were added to the plates and incubated for an hour at room temperature. Plates were washed as above, and then 25 μl of biotinylated anti-TNF (Invitrogen; clone MP6-XT3) was added a concentration of 1 μg ml^{-1} in PBS + 5% FCS for 1 h at room temperature. Plates were then washed, and 25 μl of streptavidin–HRP (Jackson ImmunoResearch) was added at a concentration of 2.5 μg ml^{-1} in 1× PBS + 5% FCS for 1 h at room temperature. Plates were then washed, assay was developed using a 50 μl of substrate reagent (R&D Systems), and absorbance was read at 450 nm.

Flow cytometry

Cells were stained with antibodies to CD11b (M1/70), SiglecF (S17007L), arginase-1 (A1exF5), iNOS (CXNFT), mertk (DS5MMER), CD64 (X54-5/7.1), CD90.2 (53-2.1), CD45.2 (104), CD45.1 (A20), B220 (RA3-6B2), CD38 (NIMR5), IgD (11-26c.2a), CD4 (GK1.5), CD95 (Jo2), GL7 (GL7), IgG1 (RMG1-1), IgA (C10-1), IgM (11/41), IL-4 (11B11), IL-17A (TC11-18H10.1), IFNγ (XMG1.2), TCRβ (H57-597), CD44 (IM7), TLR4 (SA15-21), IL-4Rα (I015F8), GXM (18B7) (from Biolegend, BD Biosciences or eBiosciences). All antibodies were used at a 1:200 dilution, except for anti-GL7 (1:400) and anti-CD11b (1:400). To detect intracellular arginase-1 or iNOS, cells were treated with BD Cytofix Buffer and Perm/Wash reagent (BD Biosciences) and then stained with anti-arginase-1 or anti-iNOS in Perm/Wash buffer. For flow cytometry on lung samples, mice were infected or challenged as indicated and then lungs were dissected and minced using scissors. The minced lung tissue was then incubated for 30 min at 37 °C in digestion medium (RPMI, 2% FCS, 0.125 mg ml^{-1} Collagenase II (Thermo Fisher Scientific), 0.2 mg ml^{-1} DNaseI (Millipore)). The digested lung tissue was then mashed through a 100-μm strainer (Fisher Scientific) and washed with RPMI + 2% FCS + 5 mM EDTA. Red blood cells were then lysed for 5 min on ice using RBC Lysis Buffer (Biolegend). Cells were resuspended in FACS buffer (1× PBS, 2% FCS, 1 mM EDTA) for staining. For analysis of mediastinal lymph nodes, the lymph nodes were dissected from mice and then mashed through a 100-μm strainer.

Expression of recombinant protein in *P. pastoris*

CPL1 was amplified by PCR from KN99α genomic DNA with a GSGS-linker–6×His tag encoded in the 3′ primer. This PCR product was then cloned into SnaBI-digested pPIC9K (Thermo Fisher Scientific) using a Gibson assembly kit (New England Biosciences). The assembled vector was transformed in to DH5α *Escherichia coli* and plated onto LB + ampicillin plates. Colonies were screened for the correct inserts by sanger sequencing (Quintara Bio). For *P. pastoris* transformation, a 50 ml culture of GS115 was inoculated overnight at 30 °C at 200 rpm. The next morning, the cultures were diluted into 500 ml YPAD and incubated (30 °C, 200 rpm) until the culture reached $A_{600} = 2.0$. Then cultures were then spun down and washed twice with ice cold 1 M sorbitol. The cells were then resuspended in 2 ml of ice-cold sorbitol

and then electroporated with 5 µg *SacI*-digested pPIC9K-CPL1-6×His. Electroporated yeast were then selected for successful integrations on -His plates.

Purification of recombinant CPL1

Single colonies were inoculated in 100 ml of BMGY (1% yeast extract, 2% peptone, 100 mM potassium phosphate pH 6.0, 1.34% YNB, 0.0005% biotin, 1% glycerol) overnight at 30 °C, 200 rpm. The next day, yeast were pelleted, washed with ddH_2O and then resuspended to A_{600} = 1.0 in BMMY (1% yeast extract, 2% peptone, 100 mM potassium phosphate pH 6.0, 1.34% YNB, 0.0005% biotin, 1% methanol) for induction. Supernatants from BMMY induction cultures (24 h at 30 °C, 300 rpm) were concentrated using 10 kD cutoff Centricon Plus −70 concentrators (EMD Millipore). The concentrated supernatants were then dialysed for 24 h (10 mM Phosphate buffer pH 7.4, 500 mM NaCl, 10% glycerol) using 30 ml 10 kD pore Slide-a-Lyzer Dialysis cassettes (Thermo Fisher Scientific). The dialysed supernatants were then run over a 5 ml HisTrap HP column using an ÄKTA pure fast protein chromatography system (Cytiva). The column was equilibrated with 25 ml of equilibration buffer (10 mM Phosphate buffer pH = 7.4, 500 mM NaCl, 10% glycerol, 20 mM imidazole) and then the dialysed supernatants were injected onto the column. The column was then washed with 25 ml of equilibration buffer. The bound proteins were then eluted in 15 ml of elution buffer (10 mM phosphate buffer pH 7.4, 500 mM NaCl, 10% glycerol, 500 mM imidazole). The eluted proteins were concentrated using 10 kD cutoff Amicon Ultra-15 Centrifugal Filter units (EMD Millipore) and then further purified on a HiLoad 16/600 Superose 6 pg preparative size-exclusion chromatography (SEC) column (GE Healthcare). The SEC column was first equilibrated with 128 ml of equilibration buffer (10 mM Phosphate buffer pH 7.4, 125 mM NaCl, 10% glycerol) and then the loaded 1 ml sample was injected, and fractions were collected over a 128 ml elution volume. The eluted fractions were run on a 4–12% SDS–PAGE (Fisher Scientific) gel and analysed by silver stain and western blot for purity. Fractions containing pure CPL1–His_6 were then concentrated to 2 mg ml^{-1} using 10 kDa cutoff Amicon Ultra-4 Centrifugal Filter units (EMD Millipore). Potential endotoxin was removed from the samples using a High Capacity Endotoxin Removal Resin (Pierce) and endotoxin levels were confirmed to be below 0.05 EU ml^{-1} using an LAL Chromogenic Endotoxin Quantification Kit (Pierce).

RNA-seq

Two-million BMDMs were seeded in six-well plates and stimulated with the indicated conditions. RNA was then extracted from the macrophages using a RNeasy Midi Kit (Qiagen). Sequencing libraries were prepared using 500 ng of purified RNA using a QuantSeq 3′ end mRNA-Seq Library Prep Kit (Lexogen). Library quality and quantify was determined using a High Sensitivity DNA Bioanalyzer chip (Agilent). The RNA-seq libraries were then sequenced using 50 bp single end reads on a HiSeq4000 (Illumina).

RNA-seq analysis

Read counts were determined using HTSeq by counting the number of reads aligned by STAR for each mouse transcript. We then used DEseq2 to determine differentially expressed genes between different treatment conditions.

Screening the *Cryptococcus* knockout collection

Individual Cryptococcus knockout strains were spotted onto YPAD + NAT omni-trays in a 96-well pattern (Thermo Fisher Scientific) from frozen −80 °C stocks. Each mutant was then inoculated into 100 µl of YPAD in 96-well round bottom plates and incubated overnight at 30 °C on a shaker. The A_{600} was then determined for each well using a plate reader, and yeast were diluted into complete DMEM at a concentration of 1×10^7 cells per ml. One-hundred microlitres of each mutant was then added to BMDMs (10^5 cells) seeded in 96-well plates. Infections were left for 24 h, and then the cells were surface stained for CD11b to distinguish macrophages from yeast, and then intracellular argainse-1 staining was performed as described above. The screen was performed over several rounds of experiments, with an average of five knockout plates screened per experiment. For each experiment, a 96-well plate of entirely wild-type *Cryptococcus* was inoculated and added to macrophages. *Z*-scores for the mutants in each experiment were calculated using the mean and standard deviation for arginase-1 induction by the wild-type plate.

Western blotting

BMDMs were stimulated with the indicated conditions and then supernatants were aspirated and cells were washed with ice cold 1× PBS. The cells were then placed on ice and lysed for 20 min in RIPA buffer (50 mM Tris-HCl pH 7.4, 150 mM NaCl, 1% NP-40, 0.5% deoxycholate, 0.1% SDS) plus protease/phosphatase inhibitor cocktail (Thermo Scientific). The lysate was then transferred to 1.5 ml Eppendorf tubes and centrifuged for 20 min at 14,000 rpm at 4 °C. Novex NuPAGE LDS samples buffer (Thermo Fisher Scientific) was then added and samples were run on 4–12% NuPAGE Bis-Tris protein gels (Thermo Fisher Scientific) at 190 V. Gels were then transferred onto nitrocellulose membranes at 35 V for 90 min. Membranes were blocked for 1 h in 5%(w/v) milk in TBST. Primary antibodies were then added at 1:1,000 in TBST + 5% mil overnight at 4C. Antibodies were used against Stat6 (D3H4), pStat6-Tyr641 (D8S9Y), Stat3 (79D7), pStat3-Tyr705 (D3A7) (all purchased from Cell Signaling Technologies). Membranes were then washing 3 × 5 min using TBST and secondary anti-rabbit horseradish (Bio-Rad) peroxidase was added at 1:10,000 for 1 h at room temperature. Membranes were washed as above and then developed for 5 min using a SuperSignal West Pico Plus Chemiluminescent Substrate kit (Fisher Scientific).

Phospho-flow cytometry

BMDMs were seeded in 6-well plates (2×10^6 cells per well) and stimulated with the indicated conditions. 16% PFA was added to each well dropwise to a final concentration of 1.5% PFA. Cells were then allowed to fix at room temperature for 10 min. The cells were then placed on ice, supernatant aspirated, and washed twice with ice cold 1× PBS. Next, the PBS was aspirated and 1 ml of ice-cold methanol was added dropwise to each well. Cells were left overnight in a −80 °C freezer. Cells were then washed twice with FACS buffer, scraped off the plate, and transferred to round bottom 96-well plates. Next, the samples were blocked at 1 h at room temperature in blocking buffer (FACS buffer + Fc Block (1:100) + FCS (1:20)). Cells were then washed with FACS buffer and stained with the indicated primary antibodies (1:100) at room temperature for 45 min. Samples were then washing twice with FACS buffer, and stained for 1 h with anti-rabbit PE (1:400) at room temperature. Finally, cells were washed twice with FACS buffer and analysed on a flow cytometer.

LDH release assay

One-hundred thousand BMDMs were seeded in 96-well plates and then stimulated with the indicated conditions in DMEM without phenol red (Corning). Supernatants were then collected and LDH release was determined using a LDH Cytotoxicity Assay kit (Fisher Scientific) in 96-well plates. The assay was then measured by absorbance at 490 nm. The percent LDH release was determined by comparing to positive control samples that were macrophage RIPA buffer lysates.

Total nitric oxide assay

One-hundred thousand BMDMs were seeded in 96-well plates and then stimulated with the indicated conditions. Supernatants were then assayed for nitric oxide in 96-well plates using a colorimetric Total Nitric Oxide Assay Kit (Thermo Fisher Scientific). Assays were read on a plate reader at an absorbance of 540 nm.

India ink capsule staining

C. neoformans single colonies were picked from YPAD plates and grown overnight in YPAD at 30 °C with shaking. The next day, cultures were

diluted 1:100 in capsule induction medium (10% Sabouraud, 50 mM HEPES pH 7.9) and incubated overnight at 30 °C with shaking. Yeast cells were then fixed with 2% paraformaldehyde for 15 min at room temperature, and washed twice with 1× PBS. Cells were resuspended in 100 µl of 1× PBS and then diluted 1:1 with India ink. Cells were then placed on slides with coverslips and imaged with a 40X objective lens using brightfield microscopy (Leica).

RT–qPCR

C. neoformans was cultured in the indicted medium and temperatures until reaching A_{600} = 1.0. Yeast were then pelleted, resuspended in 1 ml Trizol (Thermo Fisher Scientific), and lysed using a bead beater (2 cycles × 90 s). Two-hundred microlitres of chloroform was then added and the suspension was vortexed until homogenous and centrifuged at 12,500*g* at 4 °C. The aqueous phase was then collected and RNA was further extracted using an RNA Extraction Kit (Zymo Research). Reverse transcription was then performed on 5 µg of RNA using a SuperScript III Reverse Transcription Kit (Thermo Fisher Scientific). Quantitative PCR was then run with PowerUP SYBR Green Master Mix (Life Technologies) to determine the expression of *CPL1* (forward: 5′-CTCGCAGACTGGTTCAAGGT-3′; reverse: 5′-GCGCAATCTTGGCCAGAAC-3′) relative to *ACT1* (forward: 5′-CCACCCACTGCCCAAGTAAA-3′;reverse:5′-GTCGAGGGCGACCAACAATA-3′).

Reporting summary

Further information on research design is available in the Nature Research Reporting Summary linked to this paper.

Data availability

The primary read files as well as expression count files for RNA-seq data in this paper are available to download from the Gene Expression Omnibus under accession number GSE203483. Source data are provided with this paper.

42. Chun, C. D. & Madhani, H. D. Applying genetics and molecular biology to the study of the human pathogen *Cryptococcus neoformans*. *Methods Enzymol.* **470**, 797–831 (2010).

Acknowledgements We thank G. Barton for provision of *Tlr2*$^{-/-}$, *Tlr4*$^{-/-}$ and *Tlr2*$^{-/-}$*Tlr4*$^{-/-}$ mice, and R. Ricardo-Gonzalez for provision of *Il4ra*$^{-/-}$ and *Stat6*$^{-/-}$ mice; S. Chou for advice on protein purification; J. Cyster and E. Goldberg for critically reading the manuscript, discussions and advice; and S. Catania and M. Boucher for discussions and advice. Support was provided by the Chan–Zuckerberg Biohub, US National Institutes of Health, Jane Coffin Childs Memorial Fund for Medical Research Fellowship and Beckman Foundation.

Author contributions E.V.D. and H.D.M. conceived and designed the project. E.V.D. and H.D.M. designed experiments and wrote the manuscript. E.V.D. performed most of the experiments (including ELISA, flow cytometry and protein purification) and analysed the generated data. S.L. performed the forward genetic arrayed screen and helped with flow cytometry experiments. A.R. helped design and perform protein purification experiments. R.F.V. and B.W.Z. provided human monocyte-derived macrophages and read and edited the manuscript.

Competing interests The authors declare no competing interests.

Additional information
Supplementary information The online version contains supplementary material available at https://doi.org/10.1038/s41586-022-05005-4.
Correspondence and requests for materials should be addressed to Hiten D. Madhani.
Peer review information *Nature* thanks Gordon Brown and the other, anonymous, reviewer(s) for their contribution to the peer review of this work.
Reprints and permissions information is available at http://www.nature.com/reprints.

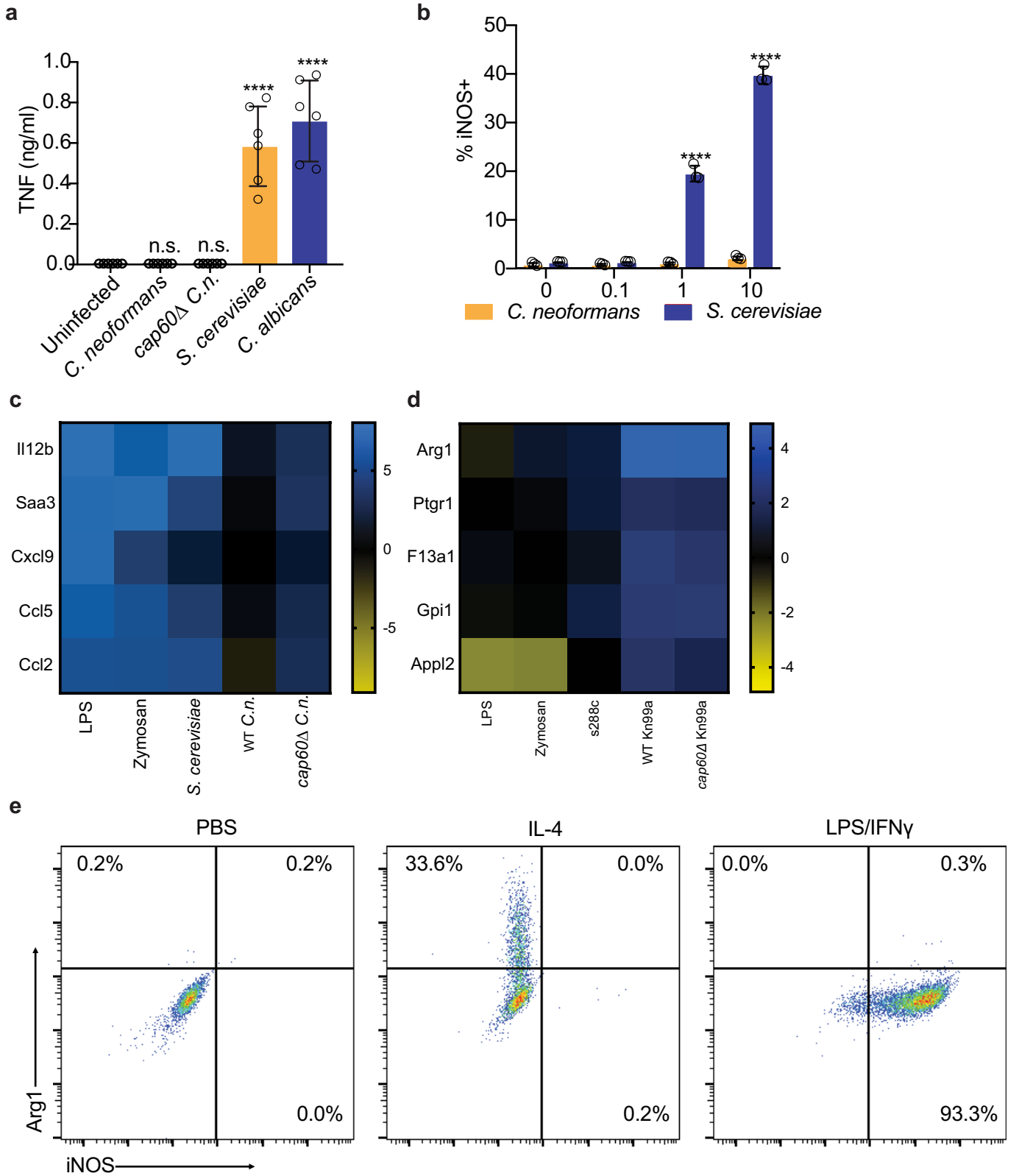

Extended Data Fig. 1 | (**a**) TNF ELISA on supernatants from BMDMs infected for 24 h with the indicated yeasts at MOI = 10. n = six biologically independent samples. Significance determined by one-way ANOVA with Bonferroni test. (**b**) Intracellular FACS staining for iNOS after 24 h of infection with either *C. neoformans* or *S. cerevisiae* at the indicated MOIs. n = three biologically independent samples. (**c**) RNA-seq heatmap depicting $\log_2$ fold changes of the indicated pro-inflammatory genes in BMDMs following 6 h of stimulation. (**d**) RNA-seq heatmap depicting $\log_2$ fold changes of the indicated M2/tolerized genes in BMDMs following 6 h of stimulation. (**e**) Representative FACS plots of ARG1 and iNOS expression in BMDMs following 24 h of stimulation with PBS, IL-4 (40 ng/ml), or LPS (100 ng/ml) and IFNγ (50 ng/ml). Data are presented as mean values +/− SD. ****$p < 0.0001$.

a

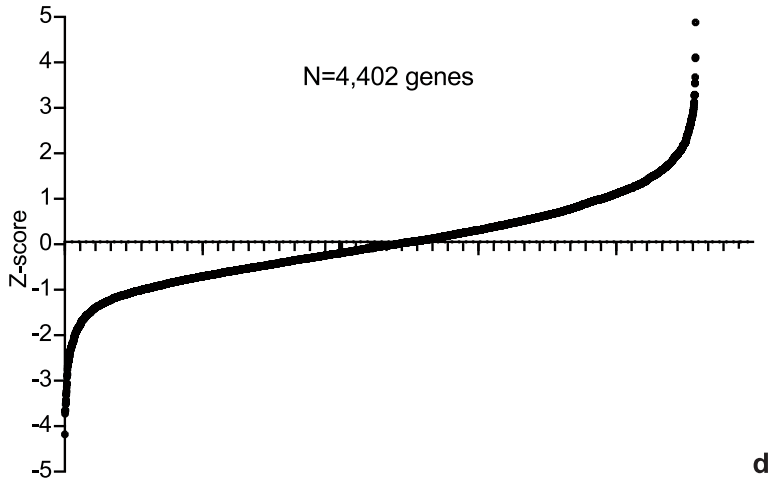

b

Gene	Description	Signal peptide?
CNAG_01551	Gat201	No
CNAG_05907	Pyruvate carboxylase	No
CNAG_03821	PI3K	No
CNAG_02797	Cpl1	Yes
CNAG_00713	V-type ATPase 54kD Subunit	No
CNAG_00560	V-type ATPase subunit E	No
CNAG_05688	V-type ATPase subunit F	No
CNAG_05162	V-type ATPase subunit E (proton transporting)	No
CNAG_04436	Hypothetical protein	No
CNAG_00131	Alcohol dehydrogenase	No
CNAG_06800	Hypothetical protein	No
CNAG_04636	Metacaspase-1	No
CNAG_03770	Hypothetical protein	No
CNAG_03025	Vacuolar ATPase Subunit D	No

c

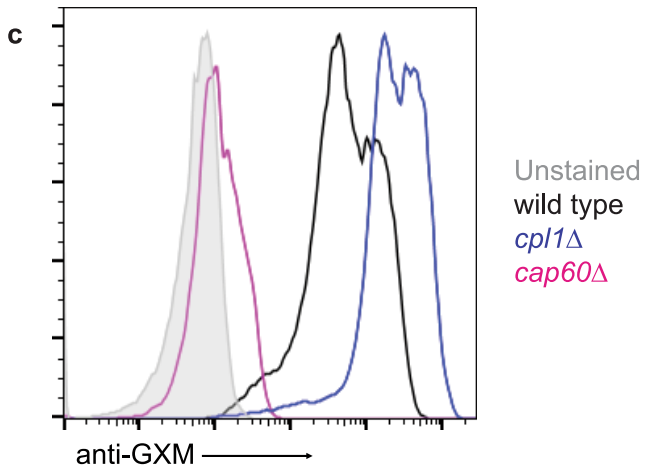

d

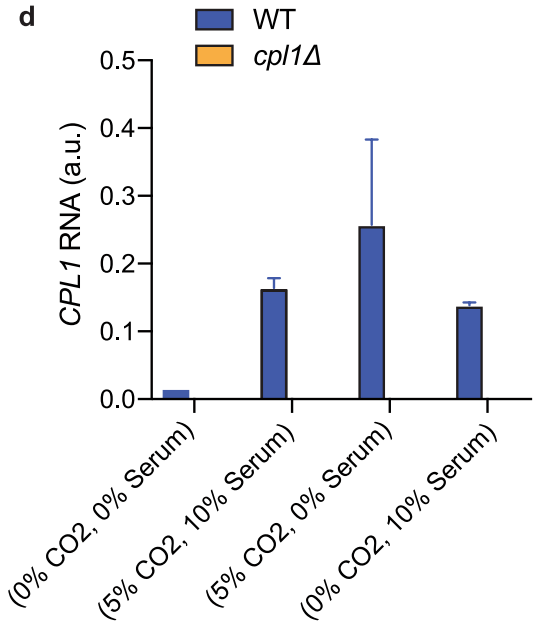

e

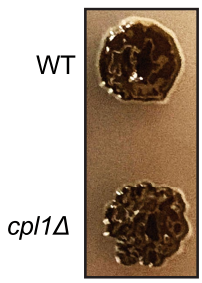

f

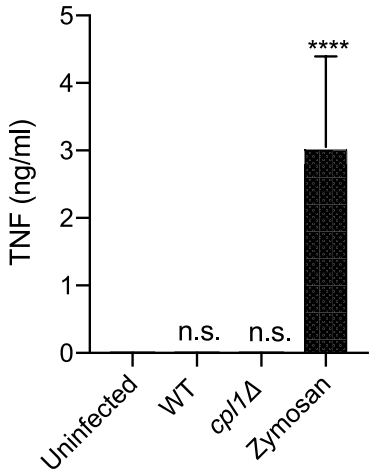

Extended Data Fig. 2 | (**a**) Ranked Z-scores of hits from forward genetic screen for *C. neoformans* Arg1 induction. (**b**) List of validated screen hits and gene descriptions. (**c**) Representative FACS histograms of GXM staining on the indicated *C. neoformans* strains cultured overnight in 10% Sabouraud media. (**d**) RT-qPCR for CPL1 mRNA expression in cultures grown to OD_{600} = 1.0 in the indicated conditions (A.U. = arbitrary units relative to ACT1). n = three biologically independent samples. (**e**) Melanin production in WT or *cpl1Δ* strains grown at 30 °C on L-DOPA plates. (**f**) TNF production (measured by ELISA) to the indicated stimulations. n = six biologically independent samples. Significance determined by one-way ANOVA with Bonferroni test. Data are presented as mean values +/− SD. ****p < 0.0001.

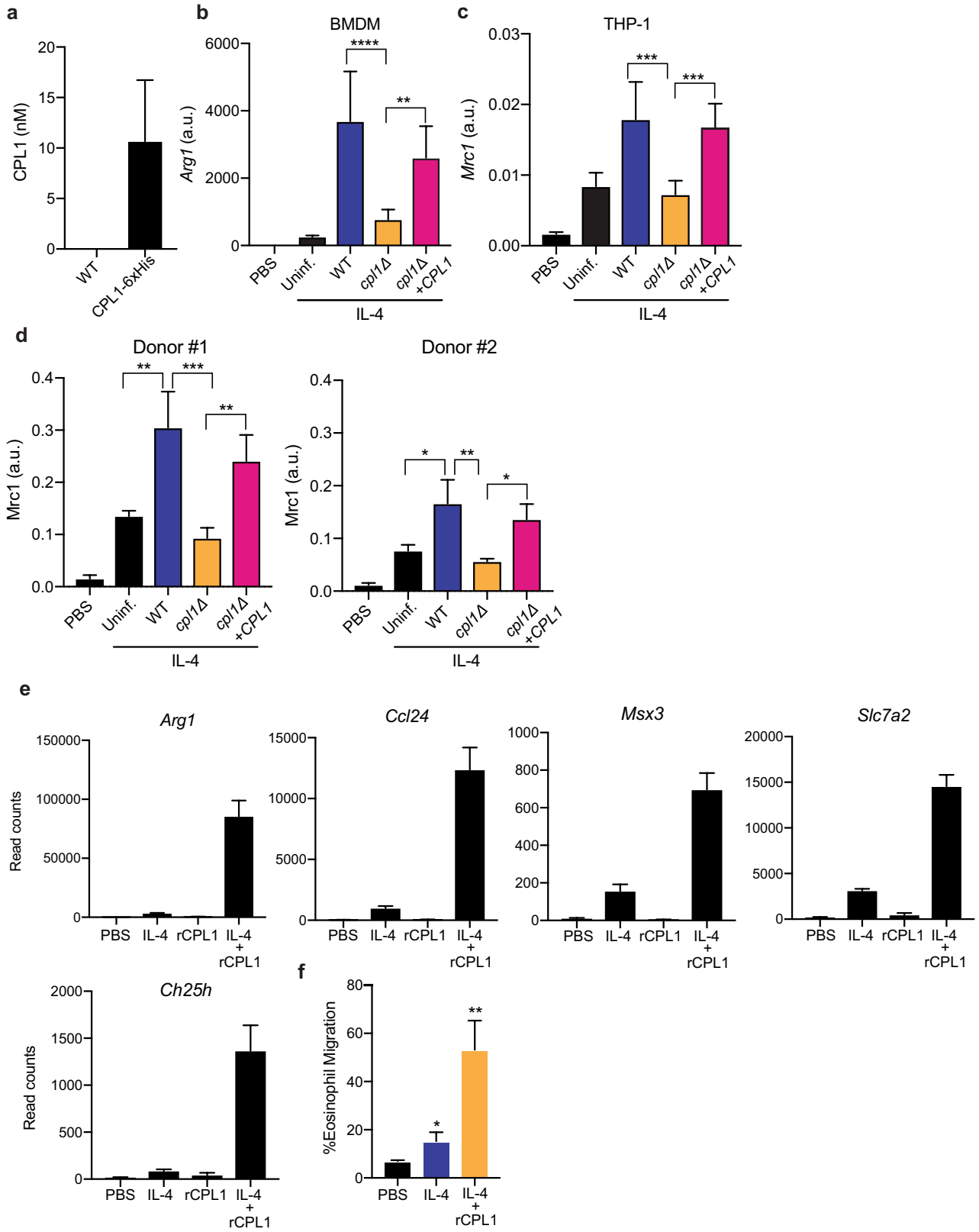

Extended Data Fig. 3 | See next page for caption.

Extended Data Fig. 3 | (**a**) Quantification by competitive ELISA of CPL1-6xHis in supernatants from the indicated strains grown in mammalian tissue culture conditions to OD = 1.0. n = six biologically independent samples. (**b**) RT-qPCR for *Arg1* mRNA in BMDMs stimulated with the indicated *C. neoformans* strains (OD = 0.1) along with IL-4 (10 ng/ml) for 24 h. Expression normalized to *Actb*, a.u. = arbitrary units. n = three biologically independent samples. (**c**) RT-qPCR for *Mrc1* mRNA in PMA-differentiated THP-1 cells stimulated with the indicated *C. neoformans* strains (OD = 0.1) along with IL-4 (10 ng/ml) for 24 h. Expression normalized to *Actb*, a.u. = arbitrary units. n = six biologically independent samples (**d**) RT-qPCR for *Mrc1* mRNA in primary human monocyte-derived macrophages stimulated for 24 h with PBS or recombinant human IL-4 (10 ng/ml) along with the indicated *C. neoformans* strains (MOI = 0.1). Expression normalized to *Actb*, a.u. = arbitrary units. n = three biologically independent samples (**e**) RNA-seq read counts of the indicated genes in BMDMs stimulated for 24 h with either PBS, IL-4 (10 ng/ml), rCPL1 (111 nM), or IL-4 + rCPL1. n = three biologically independent samples. (**f**) Transwell migration assay on splenic eosinophils towards supernatants from BMDMs stimulated as in (**e**). n = three biologically independent samples. Data are presented as mean values +/− SD.

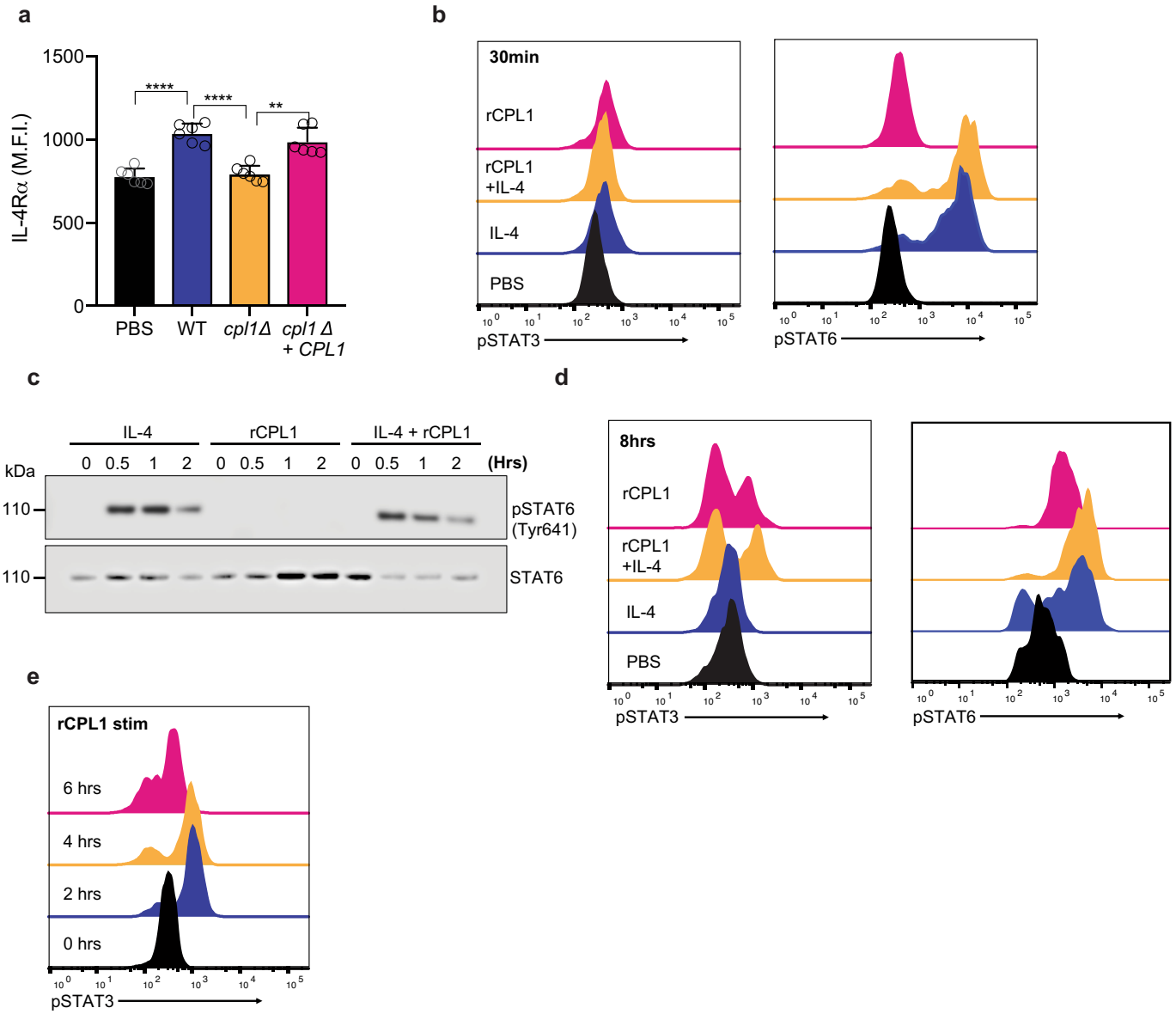

Extended Data Fig. 4 | (**a**) Representative FACS staining of surface IL-4Rα levels on BMDMs stimulated for 24 h with the indicated *C. neoformans* strains (MOI = 10). n = six biologically independent samples (**b**) Phospho-FACS for pSTAT3 (left) and pSTAT6 (right) after 30 min of stimulation with PBS, IL-4 (10 ng/ml), rCPL1 (111 nM), or IL-4 + rCPL1. (**c**) Western blot for pSTAT6 or total STAT6 on BMDMs stimulated for the indicated times with either IL-4 (10 ng/ml) alone, rCPL1 (111 nM) alone, or IL-4 + rCPL1. Data are representative of three independent experiments. (**d**) Phospho-FACS for pSTAT3 (left) or pSTAT6 (right) in BMDMs after 8 h of stimulation with PBS, IL-4 (10 ng/ml), rCPL1 (37 nM), or rCPL1+IL-4. (**e**) Phospho-FACS for pSTAT3 in BMDMs stimulated with 111 nM rCPL1 for the indicated time points. Data are presented as mean values +/− SD.

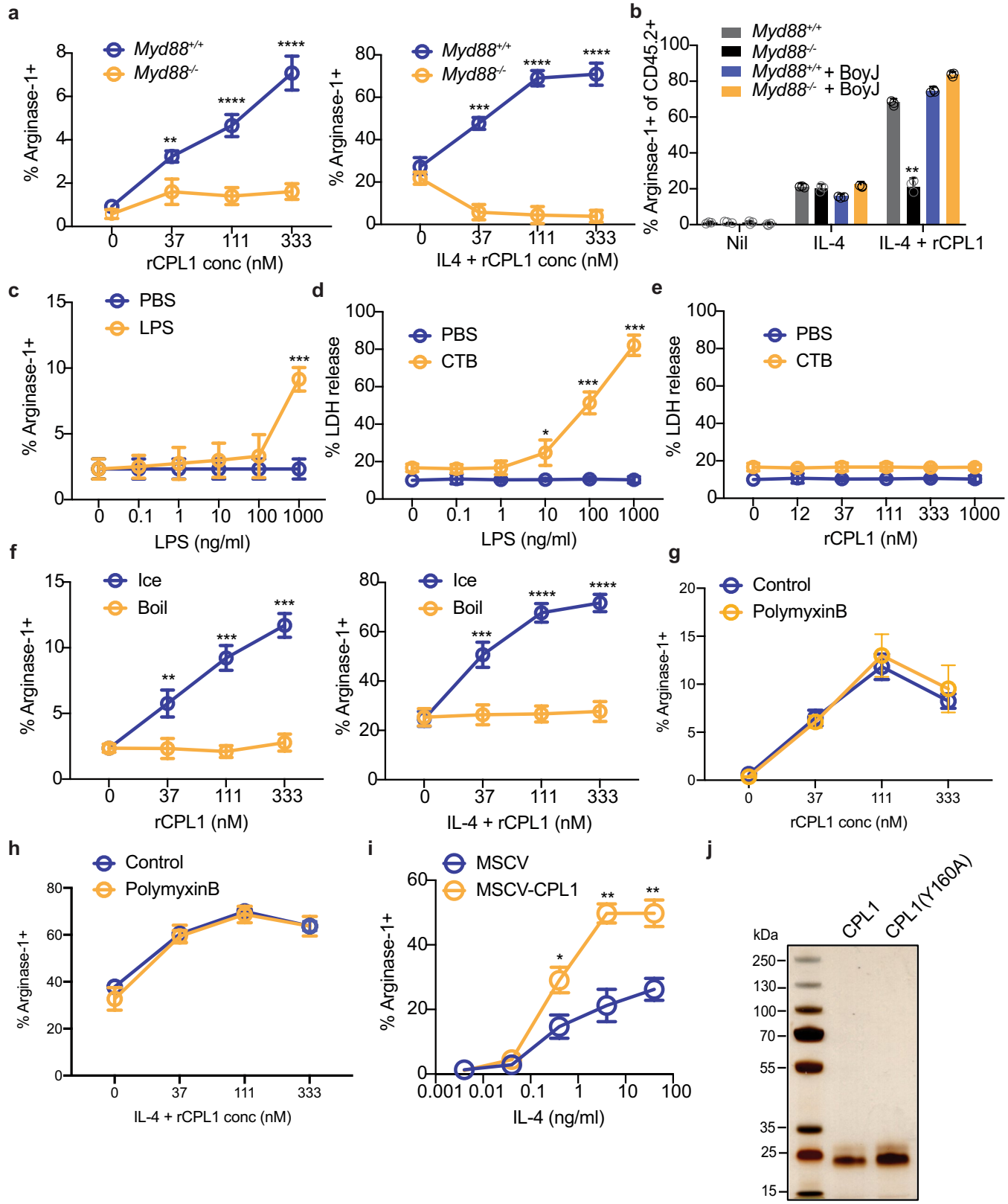

Extended Data Fig. 5 | See next page for caption.

Extended Data Fig. 5 | (**a**) Arginase-1 FACS in *Myd88*$^{+/+}$ or *Myd88*$^{-/-}$ BMDMs stimulated for 24 h with the indicated concentrations of rCPL1 alone (left) or in combination with IL-4 (10 ng/ml). n = three biologically independent samples. (**b**) Arginase-1 FACS gated on CD45.2+ BMDMs from the indicated genotypes co-cultured with a 50:50 mix of CD45.1 BoyJ BMDMs and stimulated for 24 h with IL-4 (10 ng/ml) or IL-4 + rCPL1 (111 nM). n = three biologically independent samples. (**c**) Arginase-1 FACS on BMDMs stimulated for 24 h with the indicated concentrations of LPS. (**d**) Measurement of pyroptosis by LDH release assay on BMDMs stimulated with the indicated concentrations of LPS alone or with 10 ug/ml cholera toxin B (CTB). n = three biologically independent samples. (**e**) Measurement of pyroptosis by LDH release assay on BMDMs stimulated with the indicated concentrations of rCPL1 alone or with 10 ug/ml CTB. n = three biologically independent samples. (**f**) Arginase-1 FACS on BMDMs stimulated with rCPL1 that was either kept on ice or boiled at 100 °C for 15 min. Cells were stimulated with either rCPL1 alone (left) or in combination with IL-4 (right). n = three biologically independent samples. (**g**)(**h**) Arginase-1 FACS in in BMDMs stimulated with the indicated concentrations of rCPL1 alone (**g**) or in combination with IL-4 (10 ng/ml) (**h**) that were either treated with control or polymyxinB. n = three biologically independent samples. (**i**) Arginase-1 FACS on BMDMs transduced with MSCV-empty or MSCV-CPL1 retrovirus and stimulated for 24 h with the indicated concentrations of IL-4. n = three biologically independent samples. (**j**) Silver stain on SDS-PAGE gel of rCPL1-6xHis or rCPL1(Y160A)-6xHis purified from *P. pastoris*. Image is representative of three independent experiments. Data are presented as mean values +/− SD. *p < 0.05; **p < 0.01; ***p < 0.001; ****p < 0.0001 by one-way ANOVA with Bonferroni test.

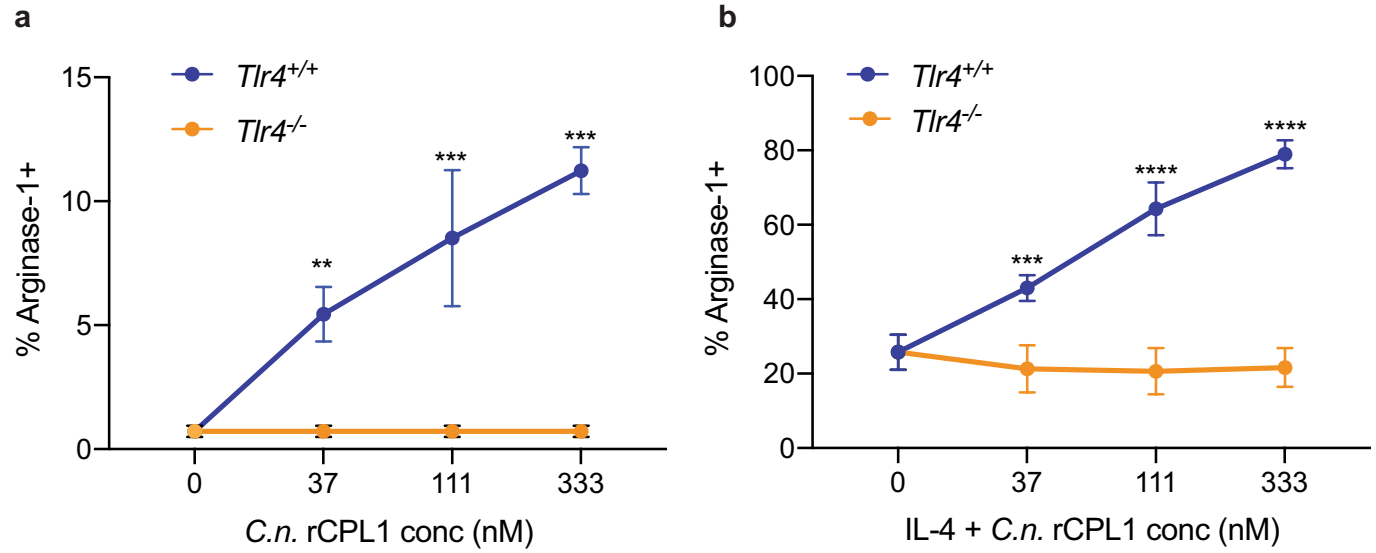

Extended Data Fig. 6 | (**a**) Arginase-1 FACS in *Tlr4*$^{+/+}$ or *Tlr4*$^{-/-}$ BMDMs stimulated for 24 h with the indicated concentrations of rCPL1-6xHis purified from *C.n.* supernatants alone or in combination with IL-4 (10 ng/ml) (**b**). n = three biologically independent samples. Data are presented as mean values +/− SD. *p < 0.05; **p < 0.01; ***p < 0.001; ****p < 0.0001 by one-way ANOVA with Bonferroni test.

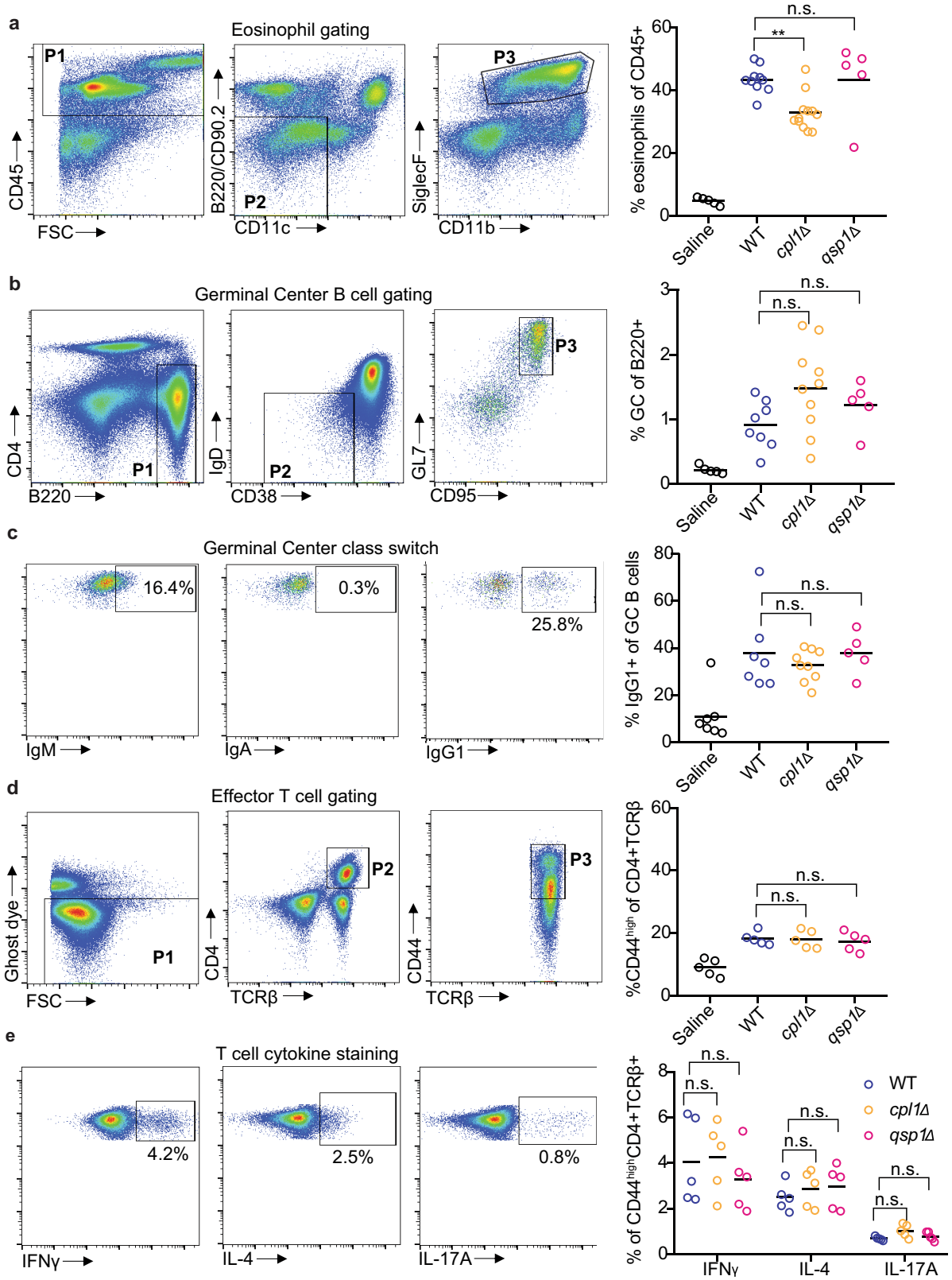

Extended Data Fig. 7 | (**a**) Representative FACS gating and quantification of lung eosinophils after 10 days of intranasal infection with the indicated *C.n.* strains. (**b**) Representative FACS gating and quantification of mediastinal lymph node GC B cells. (**c**) Representative FACS gating and quantification of GC B cell antibody isotype. (**d**) Representative FACS gating and quantification of effector CD4+ T cells. (**e**) Representative FACS gating and quantification of cytokine production from effector CD4+ T cells after 4hrs of stimulation with PMA, Ionomycin, and GolgiSTOP. **$p < 0.01$ by one-way ANOVA with Bonferroni test.

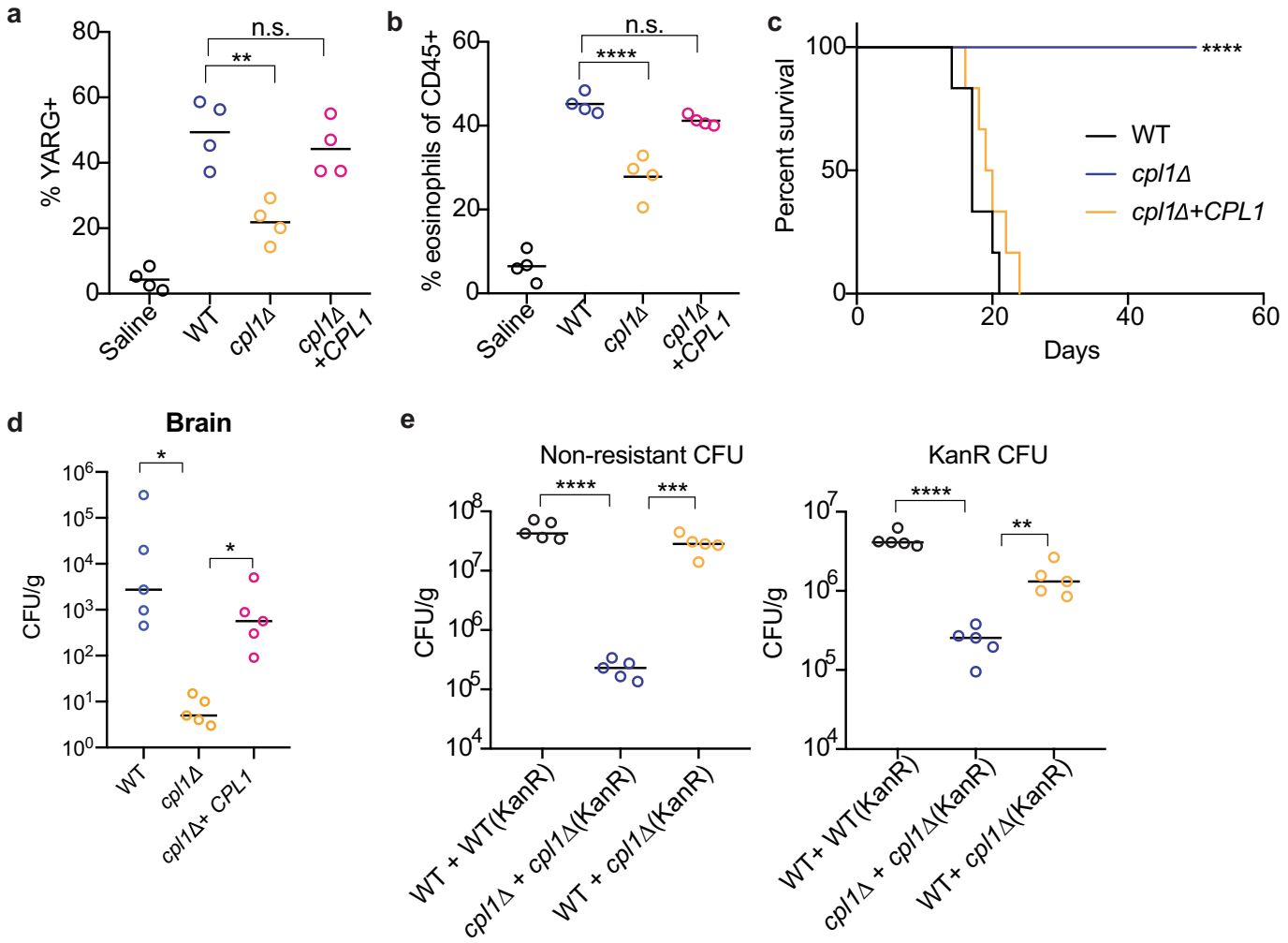

Extended Data Fig. 8 | (**a**) Quantification of YARG expression by FACS in lung interstitial macrophages in mice infected for 10 days with $5x10^4$ CFU of the indicated strains. (**b**) Quantification of eosinophils in mice infected for 10 days with $5x10^4$ CFU of the indicated strains. (**c**) Kaplan-Meier survival curve analysis of mice infected with WT, *cpl1Δ*, or *cpl1Δ+CPL1 C.n*. (N = 6 mice per group); ****$p < 0.0001$ by Mantel-Cox test. (**d**) Brain CFUs from mice infected with WT, *cpl1Δ*, or *cpl1Δ+CPL1 C.n* ($5x10^4$ CFU) for 14 days. (**e**) Lung CFUs on G418-non-resistant (left) or -resistant (right) colonies from mice infected for 10 days with a 50:50 mix of the indicated strains.

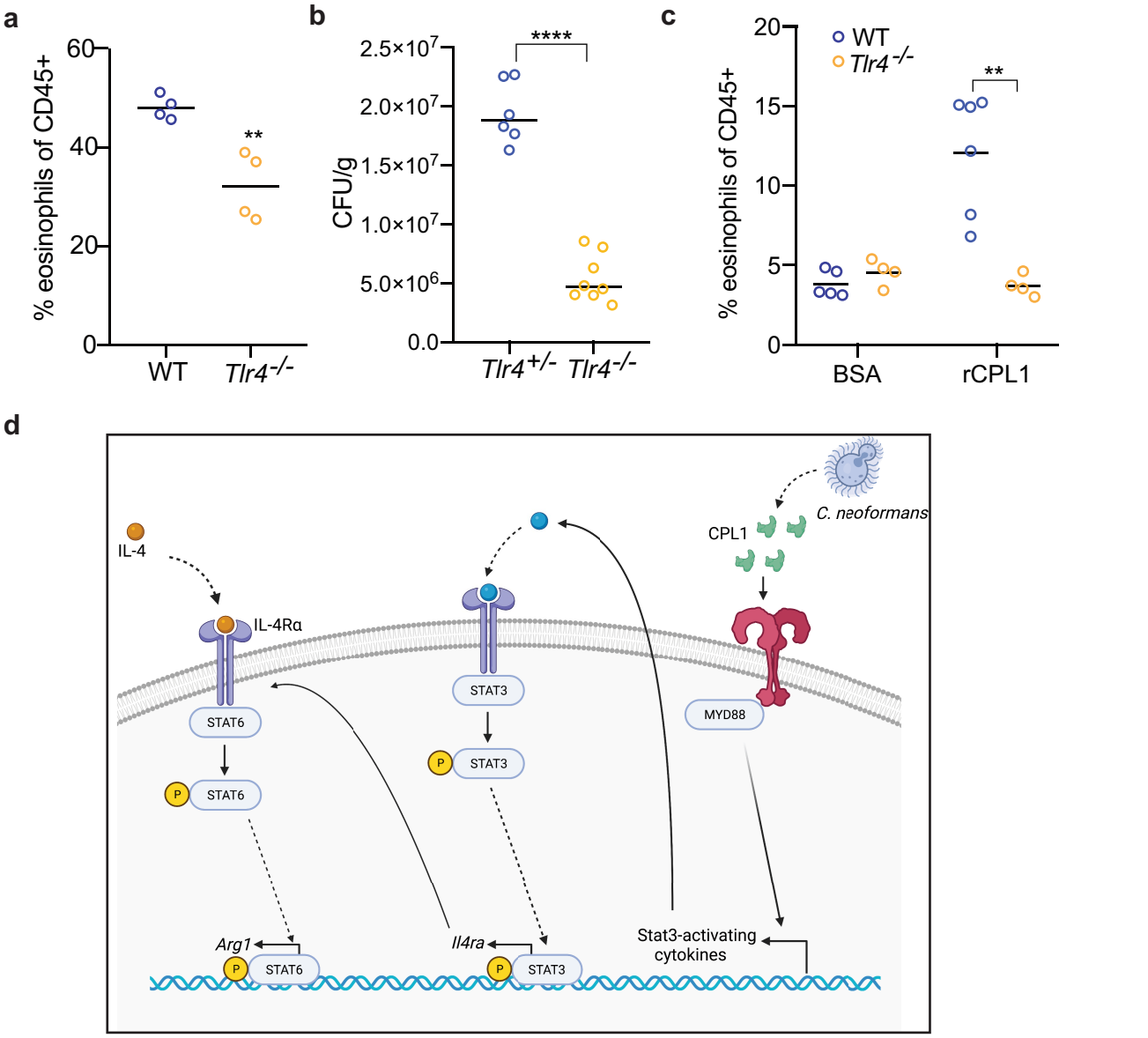

Extended Data Fig. 9 | (**a**) Quantification of lung eosinophils in WT or *Tlr4*$^{-/-}$ mice infected for 10 days with 5x10^4 CFU *C. neoformans*. (**b**) Lung CFUs from *Tlr4*$^{-/-}$ or *Tlr4*$^{-/-}$ mice infected with wild type C.n. (5x10^4 CFU) for 10 days (**c**) FACS quantification of lung eosinophils in WT (N = 6 mice) or *Tlr4*$^{-/-}$ (N = 4 mice) mice sensitized intranasally with rCPL1. (**d**) Model of how secreted CPL1 modulates the macrophage inflammatory state (created using Biorender.com). $p < 0.05$; $^{**}p < 0.01$; $^{***}p < 0.001$; $^{****}p < 0.0001$ by one-way ANOVA with Bonferroni test.

nature portfolio

Corresponding author(s): Hiten Madhani

Last updated by author(s): 2022-06-06

Reporting Summary

Nature Portfolio wishes to improve the reproducibility of the work that we publish. This form provides structure for consistency and transparency in reporting. For further information on Nature Portfolio policies, see our Editorial Policies and the Editorial Policy Checklist.

Statistics

For all statistical analyses, confirm that the following items are present in the figure legend, table legend, main text, or Methods section.

n/a	Confirmed	
☐	☑	The exact sample size (*n*) for each experimental group/condition, given as a discrete number and unit of measurement
☐	☑	A statement on whether measurements were taken from distinct samples or whether the same sample was measured repeatedly
☐	☒	The statistical test(s) used AND whether they are one- or two-sided *Only common tests should be described solely by name; describe more complex techniques in the Methods section.*
☒	☐	A description of all covariates tested
☐	☒	A description of any assumptions or corrections, such as tests of normality and adjustment for multiple comparisons
☐	☒	A full description of the statistical parameters including central tendency (e.g. means) or other basic estimates (e.g. regression coefficient) AND variation (e.g. standard deviation) or associated estimates of uncertainty (e.g. confidence intervals)
☐	☒	For null hypothesis testing, the test statistic (e.g. *F*, *t*, *r*) with confidence intervals, effect sizes, degrees of freedom and *P* value noted *Give P values as exact values whenever suitable.*
☒	☐	For Bayesian analysis, information on the choice of priors and Markov chain Monte Carlo settings
☒	☐	For hierarchical and complex designs, identification of the appropriate level for tests and full reporting of outcomes
☒	☐	Estimates of effect sizes (e.g. Cohen's *d*, Pearson's *r*), indicating how they were calculated

Our web collection on statistics for biologists contains articles on many of the points above.

Software and code

Policy information about availability of computer code

Data collection	FACS Diva v8.02
Data analysis	For RNA-seq analysis, we used open source STAR (2.7.10a) program for FastQ file alignment, HTSeq (0.11.1) for read counting, and DESeq2 (3.0) for differential expression analysis. Flow cytometry data was analyzed using FlowJo (10.7.1.) All statistics were generated using Prism 8.

For manuscripts utilizing custom algorithms or software that are central to the research but not yet described in published literature, software must be made available to editors and reviewers. We strongly encourage code deposition in a community repository (e.g. GitHub). See the Nature Portfolio guidelines for submitting code & software for further information.

Data

Policy information about availability of data

All manuscripts must include a data availability statement. This statement should provide the following information, where applicable:

- Accession codes, unique identifiers, or web links for publicly available datasets
- A description of any restrictions on data availability
- For clinical datasets or third party data, please ensure that the statement adheres to our policy

Data in this manuscript are provided as source files. RNA-seq FastQ files are available at GEO database (GSE203483).

Field-specific reporting

Please select the one below that is the best fit for your research. If you are not sure, read the appropriate sections before making your selection.

☒ Life sciences ☐ Behavioural & social sciences ☐ Ecological, evolutionary & environmental sciences

For a reference copy of the document with all sections, see nature.com/documents/nr-reporting-summary-flat.pdf

Life sciences study design

All studies must disclose on these points even when the disclosure is negative.

Sample size	The sample sizes are indicated in the figure legends. Samples sizes were ultimately determined by pooling multiple replicates done on different days and determining whether statistical significance was achieved, based on our experience and accepted practice in the field balancing statistical robustness and available resourdes. For mouse studies, individual experiments were done with a minimum of three mice per group, and each experiment was replicated multiple times.
Data exclusions	No data were excluded from this study.
Replication	All experiments were performed a minimum of three separate times with at least three biological replicates. No formal sample size analysis was performed, but the reported results were reproducible across the multiple replicates and are statistically significant based on the tests described in the text.
Randomization	For mouse studies, experiments were performed comparing litter-mate controls of the same age and sex.
Blinding	For animal studies, mice were assigned a number and the corresponding genotype was referenced in an Excel table. Genotypes were not blinded, but investigators performed harvesting and analysis based on mouse number, and genotypes were assigned after analysis was completed.

Reporting for specific materials, systems and methods

We require information from authors about some types of materials, experimental systems and methods used in many studies. Here, indicate whether each material, system or method listed is relevant to your study. If you are not sure if a list item applies to your research, read the appropriate section before selecting a response.

Materials & experimental systems

n/a	Involved in the study
☐	☒ Antibodies
☐	☒ Eukaryotic cell lines
☒	☐ Palaeontology and archaeology
☐	☒ Animals and other organisms
☒	☐ Human research participants
☒	☐ Clinical data
☒	☐ Dual use research of concern

Methods

n/a	Involved in the study
X	☐ ChIP-seq
☐	☒ Flow cytometry
X	☐ MRI-based neuroimaging

Antibodies

Antibodies used	Antibodies (Supplier, Catalogue Number, Clone): CD11b (Biolegend, 101243, M1/70), SiglecF (Biolegend, 155505, S17007L), Arginase-1 (eBioscience, 12-3697-82, A1exF5), iNOS (eBioscience, 53-5920-82, CXNFT), Mertk (eBioscience, 25-5751-80, DS5MMER), CD64 (Biolegend, 139307, X54-5/7.1), CD90.2 (Biolegend, 202529, 53-2.1), CD45.2 (Biolegend, 109819, 104), CD45.1 (Biolegend, 110729, A20), B220 (Biolegend, 103243, RA3-6B2), CD38 (BD Biosciences, 740361, NIMR5), IgD (Biolegend, 405735, 11-26c.2a), CD4 (Biolegend, 100405, GK1.5), CD95 (BD Biosciences, 557653, Jo2), GL7 (Biolegend, 144613, GL7), IgG1 (Biolegend, 406613, RMG1-1), IgA (BD Biosciences, 743298, C10-1), IgM (BD Biosciences, 743328, 11/41), IL-4 (Biolegend, 504103, 11B11), IL-17A (Biolegend, 506903, TC11-18H10.1), IFNg (Biolegend, 505807, XMG1.2), TCRb (Biolegend, 109225, H57-597), CD44 (BD Biosciences, 563736, IM7), TLR4 (Biolegend, 145403, SA15-21), IL-4Ra (Biolegend, 144804, I015F8), GXM (EMD Millipore, MABF2069, 18B7), TNF (eBioscience, 13-7326-85, 1F3F3D4), TNF (eBioscience, 14-7325-85, MP6-XT3), Stat6 (Cell Signaling Technologies, 5397S, D3H4), pStat6-Tyr641 (Cell Signaling Technologies, 56554s, D8S9Y), Stat3 (Cell Signaling Technologies, 4904T, 79D7), pStat3-Tyr705 (Cell Signaling Technologies, 9145T, D3A7), anti-rabbit horseradish peroxidase (Bio-Rad, 1706515).
Validation	See information associated with catalogue numbers: https://www.biolegend.com/, https://www.thermofisher.com/us/en/home/life-science/antibodies/ebioscience, https://www.bdbiosciences.com/en-us, https://www.emdmillipore.com/US/en, https://www.cellsignal.com/, https://www.bio-rad.com/

Eukaryotic cell lines

Policy information about cell lines

Cell line source(s)	HEK293T (ATCC), THP-1 (ATCC)
Authentication	Cell lines were purchased from ATCC but not authenticated.
Mycoplasma contamination	All cell lines tested negative for mycoplasma contamination.
Commonly misidentified lines (See ICLAC register)	No commonly misidentified lines were used in this study.

Animals and other organisms

Policy information about studies involving animals; ARRIVE guidelines recommended for reporting animal research

Laboratory animals	Mus musculus (mice) were used for animal studies and housed in a specific pathogen-free facility with a 12hour light/dark cycle. All experiments were done with both male and female mice that were 6-12 weeks old. Specific strains used in this study were: C57BL6/J, B6.SJL-Ptprca Pepcb/BoyJ, B6.129P2(SJL)-Myd88tm1.1Defr/J, B6.129-Tlr2tm1Kir/J, B6(Cg)-Tlr4tm1.2Karp/J, B6.129S4-Arg1tm1.1Lky/J, and B6.129S1-Stat3tm1Xyfu/J.
Wild animals	No wild animals were used in this study.
Field-collected samples	No field-collected samples were used in this study.
Ethics oversight	The UCSF Institutional Animal Care and Use Committee (IACUC).

Note that full information on the approval of the study protocol must also be provided in the manuscript.

ChIP-seq

Data deposition

☐ Confirm that both raw and final processed data have been deposited in a public database such as GEO.

☐ Confirm that you have deposited or provided access to graph files (e.g. BED files) for the called peaks.

Data access links *May remain private before publication.*	*For "Initial submission" or "Revised version" documents, provide reviewer access links. For your "Final submission" document, provide a link to the deposited data.*
Files in database submission	*Provide a list of all files available in the database submission.*
Genome browser session (e.g. UCSC)	*Provide a link to an anonymized genome browser session for "Initial submission" and "Revised version" documents only, to enable peer review. Write "no longer applicable" for "Final submission" documents.*

Methodology

Replicates	*Describe the experimental replicates, specifying number, type and replicate agreement.*
Sequencing depth	*Describe the sequencing depth for each experiment, providing the total number of reads, uniquely mapped reads, length of reads and whether they were paired- or single-end.*
Antibodies	*Describe the antibodies used for the ChIP-seq experiments; as applicable, provide supplier name, catalog number, clone name, and lot number.*
Peak calling parameters	*Specify the command line program and parameters used for read mapping and peak calling, including the ChIP, control and index files used.*
Data quality	*Describe the methods used to ensure data quality in full detail, including how many peaks are at FDR 5% and above 5-fold enrichment.*
Software	*Describe the software used to collect and analyze the ChIP-seq data. For custom code that has been deposited into a community repository, provide accession details.*

Flow Cytometry

Plots

Confirm that:

☐ The axis labels state the marker and fluorochrome used (e.g. CD4-FITC).

☐ The axis scales are clearly visible. Include numbers along axes only for bottom left plot of group (a 'group' is an analysis of identical markers).

☒ All plots are contour plots with outliers or pseudocolor plots.

☒ A numerical value for number of cells or percentage (with statistics) is provided.

Methodology

Sample preparation	For mouse lung tissue and mediastinal lymph nodes, tissues were collected in digestion media (RPMI + 2% FCS + 0.125mg/ml Collegenase II) and digested for 30min at 37C. Digested tissues were then mashed using 100um strainers to generate a single cell suspension. Cells were then stained with antibodies on ice in FACS buffer (1X PBS + 2% FCS + 2mM EDTA).
Instrument	BD FACSCelesta Model 660345
Software	FlowJo 10.7.1
Cell population abundance	No cell sorting was done in this work.
Gating strategy	All markers used to identify distinct cell types were clearly separated from the background intensity. In relevant experiments, FMO controls were used to determine positive gates.

☒ Tick this box to confirm that a figure exemplifying the gating strategy is provided in the Supplementary Information.

Magnetic resonance imaging

Experimental design

Design type	*Indicate task or resting state; event-related or block design.*
Design specifications	*Specify the number of blocks, trials or experimental units per session and/or subject, and specify the length of each trial or block (if trials are blocked) and interval between trials.*
Behavioral performance measures	*State number and/or type of variables recorded (e.g. correct button press, response time) and what statistics were used to establish that the subjects were performing the task as expected (e.g. mean, range, and/or standard deviation across subjects).*

Acquisition

Imaging type(s)	*Specify: functional, structural, diffusion, perfusion.*
Field strength	*Specify in Tesla*
Sequence & imaging parameters	*Specify the pulse sequence type (gradient echo, spin echo, etc.), imaging type (EPI, spiral, etc.), field of view, matrix size, slice thickness, orientation and TE/TR/flip angle.*
Area of acquisition	*State whether a whole brain scan was used OR define the area of acquisition, describing how the region was determined.*

Diffusion MRI ☐ Used ☐ Not used

Preprocessing

Preprocessing software	*Provide detail on software version and revision number and on specific parameters (model/functions, brain extraction, segmentation, smoothing kernel size, etc.).*
Normalization	*If data were normalized/standardized, describe the approach(es): specify linear or non-linear and define image types used for transformation OR indicate that data were not normalized and explain rationale for lack of normalization.*
Normalization template	*Describe the template used for normalization/transformation, specifying subject space or group standardized space (e.g. original Talairach, MNI305, ICBM152) OR indicate that the data were not normalized.*
Noise and artifact removal	*Describe your procedure(s) for artifact and structured noise removal, specifying motion parameters, tissue signals and physiological signals (heart rate, respiration).*

Volume censoring

Define your software and/or method and criteria for volume censoring, and state the extent of such censoring.

Statistical modeling & inference

Model type and settings

Specify type (mass univariate, multivariate, RSA, predictive, etc.) and describe essential details of the model at the first and second levels (e.g. fixed, random or mixed effects; drift or auto-correlation).

Effect(s) tested

Define precise effect in terms of the task or stimulus conditions instead of psychological concepts and indicate whether ANOVA or factorial designs were used.

Specify type of analysis: ☐ Whole brain ☐ ROI-based ☐ Both

Statistic type for inference
(See Eklund et al. 2016)

Specify voxel-wise or cluster-wise and report all relevant parameters for cluster-wise methods.

Correction

Describe the type of correction and how it is obtained for multiple comparisons (e.g. FWE, FDR, permutation or Monte Carlo).

Models & analysis

n/a	Involved in the study
☐	☐ Functional and/or effective connectivity
☐	☐ Graph analysis
☐	☐ Multivariate modeling or predictive analysis

Functional and/or effective connectivity

Report the measures of dependence used and the model details (e.g. Pearson correlation, partial correlation, mutual information).

Graph analysis

Report the dependent variable and connectivity measure, specifying weighted graph or binarized graph, subject- or group-level, and the global and/or node summaries used (e.g. clustering coefficient, efficiency, etc.).

Multivariate modeling and predictive analysis

Specify independent variables, features extraction and dimension reduction, model, training and evaluation metrics.